Ecological Indicators 159 (2024) 111696

Contents lists available at ScienceDirect

Ecological Indicators

journal homepage: www.elsevier.com/locate/ecolind

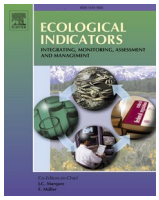

A cost-effective method to map mangrove forest extent, composition, and condition in small islands based on Sentinel-2 data: Implications for management

Gema Casal [a,*], Ewan Trégarot [b], Cindy C. Cornet [b], Tim McCarthy [a], Matthijs van der Geest [c]

[a] National Centre for Geocomputation, 2nd Floor Iontas Building, North Campus, Maynooth University, Maynooth, Kildare, Ireland
[b] Centre for Blue Governance, Department of Economics and Finance, Portsmouth Business School, University of Portsmouth, Richmond Building, Portland Street, Portsmouth PO1 3DE, United Kingdom
[c] Wageningen Marine Research, Wageningen University & Research, P.O. Box 57, 1780 AB, Den Helder, the Netherlands

ARTICLE INFO

Keywords:
Leaf Area Index
Net Primary Productivity
SL2P
Ecological condition
Coastal monitoring

ABSTRACT

Despite their ecological, economic, and social importance, mangrove ecosystems suffer from high levels of degradation caused by a combination of anthropogenic stressors and the effects of climate change. Their degradation inevitably reduces the provision of ecosystem services and ultimately impacts human well-being, especially in coastal communities of Small Islands Developing States (SIDS). To timely identify and manage stressors causing local mangrove degradation, *in situ* monitoring is required. However, the financial means and human capacity to do so are often limited in SIDS, hampering adequate management of their mangrove forests. In search of a cost-effective alternative, we evaluated the use of Sentinel-2 satellites to monitor mangrove extent and species distribution in Lac Bay, a bay located on the small tropical island of Bonaire (Caribbean Netherlands). We also evaluated the mangrove's ecological condition through two biophysical variables 1) Effective Leaf Area Index (LAI_e) and 2) Net Primary Productivity (NPP). Our results showed that Sentinel-2 data are a valuable tool for mapping the extent of mangrove forests in Bonaire and species composition (mean overall accuracy > 95 %). Using five Sentinel-2 images from 2021 and 2022, the extent of mangrove forests in Lac Bay was estimated to be on average 222.3 ha, of which 136.0 ha were classified as *Rhizophora mangle* (red mangrove) and 77.1 ha as *Avicennia germinans* (black mangrove). Mean values for predicted LAI_e ranged from 3.37 to 3.85 for Lac Bay, with significantly higher values in the wet season (3.82 ± 0.57) compared to the dry season (3.40 ± 0.56). The generic Simplified Level-2 Prototype Processor (SL2P) underestimated the LAI_e values in Lac Bay, with moderate differences between SL2P values and *in situ* data (BDE = 0.41, RMSE = 1.09). Mean NPP values were estimated to be 8.82 ± 1.46 (g Cm^{-2} d^{-1}). LAI_e and NPP maps showed a zonal distribution, with highest values in the mid-West and East on the seaward side, and lowest values in the northern landward part of Lac Bay. The method developed in this study provides a cost-effective way to monitor the extent, composition, and ecological condition of mangrove forests, which can be used by small island states to make informed decisions about the management and protection of mangrove ecosystems.

1. Introduction

The global decline of mangrove forests is concerning, as these ecosystems provide many important ecological and socioeconomic benefits, including enhanced biodiversity, coastal protection, carbon sequestration, and support of local fisheries (Bryan-Brown et al., 2020; Goldberg et al., 2020). Between 1980 and 2000, mangrove forests declined by 35 % worldwide (Millennium Ecosystem Assessment, 2005) and kept declining globally but at a slower rate of 3.4 % between 1996 and 2020 (Bunting et al., 2022). Compared to global trends, mangrove forests in the Caribbean have suffered even more damage over the last two decades, with a decline of 7.9 % between 1996 and 2020, which is mainly attributed to coastal development, demographic growth, and climate change (Bunting et al., 2022). If current rates of mangrove loss in the Caribbean are maintained, mangroves will go extinct from this region over the next three centuries (Rull, 2023).

* Corresponding author.
E-mail address: gema.casal@mu.ie (G. Casal).

https://doi.org/10.1016/j.ecolind.2024.111696
Received 25 August 2023; Received in revised form 2 February 2024; Accepted 2 February 2024
Available online 7 February 2024

The loss of these valuable ecosystems in the Caribbean has significant implications for biodiversity, coastal ecosystem resilience, and human well-being, especially for coastal communities on small island states that rely heavily on the ecosystem services provided by mangrove forests. Therefore, efforts to address mangrove loss in the Caribbean should be aligned with global conservation strategies, including protecting remaining mangrove areas, restoring degraded mangroves, and promoting sustainable management policies. However, ecological data about the condition and extent of mangrove forests are often missing, mostly due to the limited human capacity and financial means available on small islands, hampering the conservation and restoration of Caribbean mangroves (Flores de Santiago, 2013; Rull, 2023).

Field research campaigns are essential to collect data on the ecological condition of these ecosystems, but mangrove forests are challenging environments. The combination of soft sediment (mud), dense stands with complex aerial root systems under the influence of tides, along with the remoteness and inaccessibility of some areas, makes extensive sampling and long-term monitoring impractical and highly demanding in terms of human and financial resources (Green et al., 1998; Feka and Morrison, 2017). Remote sensing technology is considered a cost-effective alternative for providing long-term data on large areas of mangrove forests, including inaccessible and hazardous areas. Satellites can provide reliable information with temporal and spatial continuity, which is particularly important for small island developing states (SIDS) with limited access to geoinformation (Shrestha et al., 2019). Remote sensing has proven to be a valuable tool for studying and monitoring relatively large mangrove forests, providing important information on mangrove extent, species classification, vertical structure and biomass, carbon stock estimation, ecohydrology and climate change impacts (Wang et al., 2019). Many of these studies have used broad spatial resolution satellites such as MODIS (e.g., Barr et al., 2013; Ishtiaque et al., 2016) or VIIRS (e.g., Waiyasusri, 2021) and even the Landsat series (e.g., Green et al., 1997; Giri et al., 2011). Due to their spatial resolution (>250 m in the case of MODIS) and limited revisit time (16 days in the case of Landsat series), these satellites are not very suitable for mapping and monitoring mangrove forests in small islands, which are usually distributed along coastlines in thin fringes less than 250 m wide and which are often masked by clouds. Despite these limitations, remote sensing has been used to generate mangrove forests maps at global scales. Global Mangrove Watch (GMW) datasets include global maps of mangrove forests at 30 m of spatial resolution derived from L-band SAR (Tomas et al., 2017) and Landsat imagery (Bunting et al., 2018). However, at 30 m, small mangrove forests could still be missed (Bunting et al., 2022). Sentinel-2 satellites, operated by the European Space Agency (ESA) under the Copernicus Programme, provide new technical capabilities that appear suitable for monitoring small mangrove forests at higher scales of benefit for many small tropical islands. These satellites offer relatively high spatial resolutions (10 m in some of their bands), frequent revisit time (5 days at the equator), and free and open data policy. Recent efforts have been made to create global mangrove forests maps using Sentinel-2 data (Bunting et al., 2022; Jia et al., 2023). Nevertheless, the incorporation of diverse data sources, coupled with varied classification methods and adherence to distinct cartographic standards, are likely to lead to inconsistent outcomes. Moreover, while global maps are generated at particular moments in time, the temporal dynamics crucial for ongoing monitoring and analysis are often absent from these outputs.

Leaf Area Index (LAI) is a crucial parameter of vegetation structure and provides important information about the proportion of leaf area per unit ground area in a vegetation canopy (Chen and Black, 1992). LAI is often used as a proxy for total leaf biomass and vegetation productivity and is closely related to other ecological processes (Lu et al., 2017). For example, leaves affect the amount of water transpired by vegetation and can also impact nutrient cycling by influencing the amount of litterfall and litter decomposition rates, which in turn affect nutrient availability to the ecosystem. In addition, LAI is an important parameter in ecosystem models, often used as an input parameter for estimating energy and water balance and other ecosystem processes (Yan et al., 2012). As a result, LAI has been defined as an Essential Climate Variable (GCOS, 2011). One of the most widely used global LAI products is the MODIS sensor-derived product, which has a spatial resolution of 500 m (Myneni et al., 2015) and include archive data since 2000. More recently, the Copernicus Global Land Service has begun to produce LAI products with a spatial resolution of 300 m (De Grave et al., 2021) including data from January 2014 to present. However, these spatial resolutions are too broad to monitor the ecological condition of small mangrove forests, like those present on small islands. The steep slopes of volcanic islands and/or the microtidal range give little space for mangroves to develop, often forming a small stretch along the coastline. Landsat satellites with a spatial resolution of 30 m have also been used to derive LAI (Gao et al., 2012), but their revisit time of 16 days reduces the number of suitable images in areas frequently covered by clouds, which is the case for most islands in the tropics. The Copernicus mission Sentinel-2, currently comprising of two twin satellites on operation Sentinel-2A (launched in 2015) and Sentinel-2B (launched in 2017), offers new opportunities to map LAI in small mangrove forests. Yet, while several studies have indeed proven that Sentinel-2 satellites can be an effective tool for deriving LAI in large mangrove forests in Asian countries such as China (Guo et al., 2021), Vietnam (Binh et al., 2022) and India (Parida and Kumari, 2021), no such studies seem available for small mangrove forests, such as those found on small islands in the Caribbean Sea.

Net Primary Productivity (NPP) is another important parameter for understanding ecological dynamics and carbon budgets of mangrove forests. NPP refers to the net carbon gain by vegetation over a particular period. It corresponds to the balance between carbon absorbed by photosynthesis and carbon released by plant respiration. NPP can be used as the main assessment factor in studies of regional carbon flux and regulation of ecological processes (Field et al., 1998). However, measuring this parameter is challenging because there are many sources of error. Some authors reported that most field measurements underestimate actual NPP by at least 30 % (Chapin and Eviner, 2003). As NPP cannot be measured directly at regional or global scales, it is usually inferred by models (e.g., Piao et al., 2001). The use of remote sensing has improved the capabilities for NPP estimations due to the spatial and temporal continuity of the data, allowing large mangrove areas to be covered cost-effectively. Several models have been developed to estimate NPP using remote sensing data (Goetz et al., 2000; Pachavo and Murwira, 2014). Although satellite data have been used to monitor NPP in mangrove forests (e.g., Ishtiaque et al., 2016; Azhdari et al., 2020), the number of studies is lower than for other vegetation types, so that developments for its application in mangrove forests still lag behind. Moreover, as is the case for LAI, products such as the MODIS NPP (MOD17A3) with a spatial resolution of 1 km are too coarse for small mangrove forests. With a spatial resolution of 10 m and a revisit time of 5 days, the freely available images from Sentinel-2 satellites also provide a great opportunity for monitoring NPP of small mangrove forests, as often present on small islands in the Caribbean, but to our knowledge this has not been studied so far.

This study aims to provide a cost-effective method for monitoring the extent and ecological condition of small mangrove forests (<300 ha) that can be used by small island states, with often limited access to resources and capacity particularly in the Caribbean, to make informed decisions about management and protection of these valuable ecosystems. In this context, the present study will 1) evaluate the use of Sentinel-2 satellite images for mapping the extent and species composition of small mangrove forests on Bonaire, a small Caribbean island and 2) validate and develop LAI and NPP products derived from Sentinel-2 images to assess mangrove forests ecological condition and their impact on climate regulation.

2. Material and methods

2.1. Study area

Bonaire (Caribbean Netherlands) is a small island in the Caribbean Sea, located around 87 km north of Venezuela, with a land area of 288 km^2 (Fig. 1). The population of Bonaire reached 21,745 residents on 1 January 2021 (CBS, 2021). The climate is semi-arid and tropical, with little seasonal variation and average monthly air temperatures between 26.6 °C (February) and 28.4 °C (October) (De Meyer, 1998). The dry season runs from February to August, and the wet season runs from October to January, with August and September as transition months towards the wet season (Dullaart and van Mannen, 2022). The current annual rainfall is ~ 500 mm (Slijkerman et al., 2019) but this amount is expected to decrease by 5 % to 6 % by the end of the century (IPCC, 2013).

Lac Bay, located on the southeast coast of Bonaire, forms part of the Bonaire National Marine Park and has been declared a RAMSAR site since 2003 (Fig. 1). The tidal range within the bay is limited to about 0.3 m (van Moorsel and Meijer, 1993) and combined with the shallow nature of the bay (mostly 0–3 m deep) translates into limited circulation. In combination with daily evaporation of 8.4 mm for fully sun-exposed open water (De Freitas et al., 2014), this limited water circulation has resulted in hypersaline conditions in the shallow Northern backwaters in the bay (Debrot et al., 2019). Lac Bay contains the most important mangrove populations on Bonaire and is considered the largest mangrove area in the former Netherlands Antilles (Wösten, 2013). The predominant mangrove species are *Rhizophora mangle* (red mangrove) and *Avicennia germinans* (black mangrove), while *Laguncularia racemosa* (white mangrove) is also known to be occasionally present (Davaasuren and Meesters, 2012). While *A. germinans* grows in muddy and highly saline sediments in the northern area (De Freitas et al., 2005; Davaasuren and Meesters, 2012), *R. mangle* grows in more permanently flooded areas towards the lagoon.

The mangrove system of Lac Bay exhibits a non-estuarine nature, which is common on small islands where freshwater run-off is absent (Nagelkerken, 2007).

2.2. Fieldwork campaigns

In the case of canopies with a random distribution of foliage, LAI can be determined by assessing the likelihood that a beam of direct radiation passes through the canopy without obstruction (Gower et al., 1999). This probability aligns with the principles of the Beer-Lambert Law (Nilson, 1971; Gower et al., 1999). Following this principle, Effective Plant Area Index (PAI_e) was derived by indirect optical ground-based measurements using a handheld digital lux meter (HoldPeak HP-8801C, Range: 1–400 000 Lux; Resolution: 0.1 Lux/Fc) (DES, 2018).

In situ PAI_e data were collected at 51 haphazardly selected sites in Lac Bay between 23 September and 29 October 2021 (n = 3) and between 5 March and 24 May 2022 (n = 48), covering a range of different ecological conditions (Fig. 2,3a; Table 1). In 2021, a 10 m by 10 m plot was haphazardly selected at each sampling site to characterise the forest structure (Fig. 2a). Within each plot, canopy height (m) and species

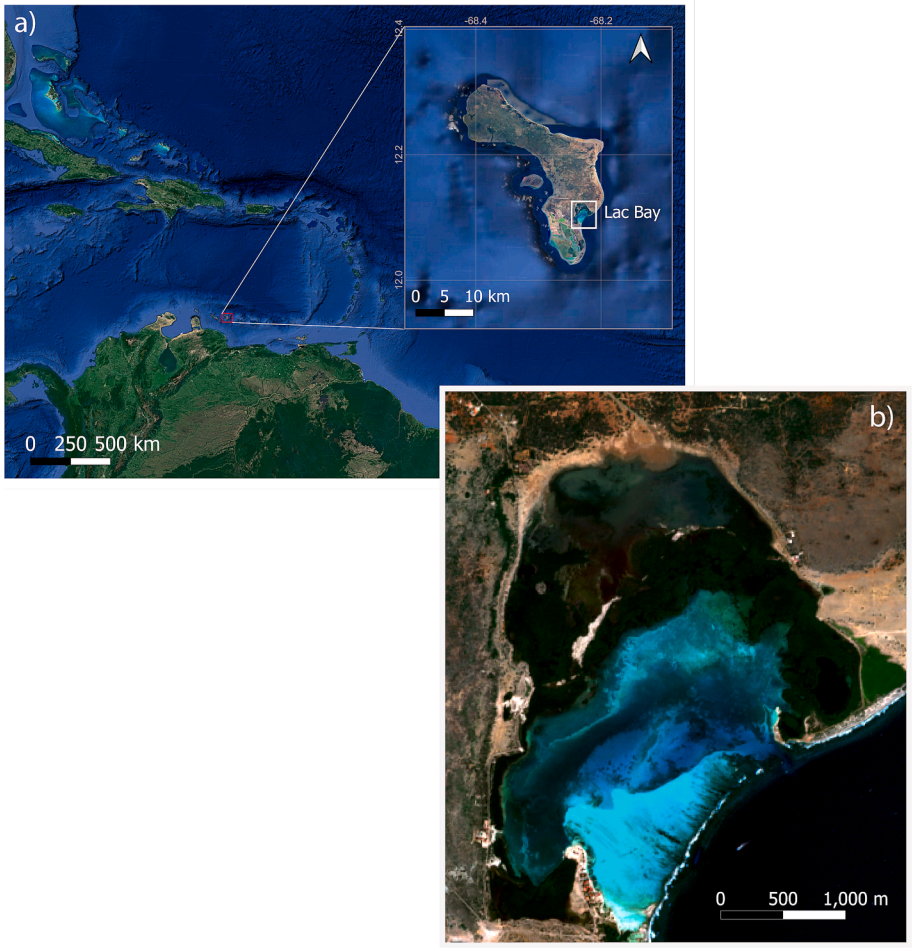

Fig. 1. (a) Map showing the location of Lac Bay on Bonaire within the wider Caribbean region (Source: Google Earth imagery). (b) Sentinel-2 image (RGB) of Lac Bay registered on 28/12/2021.

Fig. 2. Photos taken during field campaigns to assess different variables of mangrove forest structure in Lac Bay, Bonaire. (a) Laying out a transect line to define a sampling quadrat. (b) Some sampling stations needed to be accessed by boat. (c) Taking light measurements underneath the mangrove canopy using a digital luxmeter. Photo credits: Cindy Cornet (a); Humming Drone HD-Prod (b,c).

Table 1
Fieldwork dates and number of sites where PAI_e measurements were made.

Fieldwork Date	Number of sites (n)
23/09/2021	2
29/09/2021	1
11/03/2022	13
16/03/2022	9
23/03/2022	1
31/03/2022	1
06/04/2022	1
12/04/2022	2
14/04/2022	1
22/04/2022	2
28/04/2022	2
04/05/2022	2
06/05/2022	5
10/05/2022	1
13/05/2022	3
19/05/2022	1
21/05/2022	3
24/05/2022	1

composition were visually assessed. If tree density was too high in the plot, the plot size was reduced to 5 m x 5 m, which also was the plot size used in 2022. A minimum of 19 light readings were taken within each plot by walking along its boundaries and taking a light reading at roughly every meter in addition to a series of random readings taken inside the plot (Fig. 2c). Moreover, a minimum of 3 additional light readings were taken in direct sunlight in the nearest open space adjacent to the study plot right before and just after light readings within each plot. This process was done to assess the mean light intensity in direct sunlight as a proxy of the light intensity above the canopy. All light readings were done between 09:00 and 16:00 on sunny days.

In situ PAI_e was derived by calculating the ratio of mean light intensity within the plot to the mean light intensity in direct sunlight using the following equation (adapted from DES, 2018):

$$PAI_e = \frac{Ln\left(\frac{l_b}{l_0}\right)}{-k \cdot cos\left(\frac{\infty \pi}{180}\right)} \quad (1)$$

where Ln = Natural logarithm, l_b = Mean value of light below the canopy, l_0 = Mean value of light above the canopy, k = Extinction coefficient that accounts for the angle and orientation of the foliage (a k value of 0.55 has been chosen, which is appropriate for mangrove stands according to Clough et al., 1997), ∞ = Zenith angle of the sun and π = 3.14. NOAA solar calculation (https://gml.noaa.gov/grad/solcalc/calcdetails.html) was used to retrieve the zenith angle based on the coordinates of the quadrats and the date and time of the measurements.

PAI_e includes both the leaf area and the woody material. For this reason, PAI_e was converted into effective Leaf Area Index (LAI_e) by applying a first-order correction for woody material (Chen et al., 1996):

$$LAI_e = (1 - \alpha) \cdot PAI_e \quad (2)$$

where α is the woody-to-total-plant-area ratio, used to represent the contribution of woody material to the total area, including non-green leaves, branches, and tree trunks.

The range of typical values of wood-to-total-plant areas ratio differs between vegetation types. Considering the mangrove forest as a broadleaf forest, a value of 0.2 was selected for α (Gower et al., 1999). An additional field campaign was performed on 14 March 2023 to identify homogenous areas of *A. germinans* and *R. mangle*. For this purpose, several GPS tracks were made, defining twelve monospecific areas, five for *R. mangle* with a total area of 2.98 ha and seven for *A. germinans* with a total area of 2.47 ha (Fig. 3b).

2.3. Sentinel-2 imagery

Both Sentinel-2A and Sentinel-2B satellites have a single multispectral instrument (MSI) onboard that can acquire optical images in 13 spectral bands from Visible and Near Infrared (VNIR) to Shortwave Infrared (SWIR) with spatial resolutions of 10 m, 20 m, and 60 m (Drusch et al., 2012). Although primarily designed for terrestrial observation, the Sentinel-2 mission covers coastal waters up to 20 km

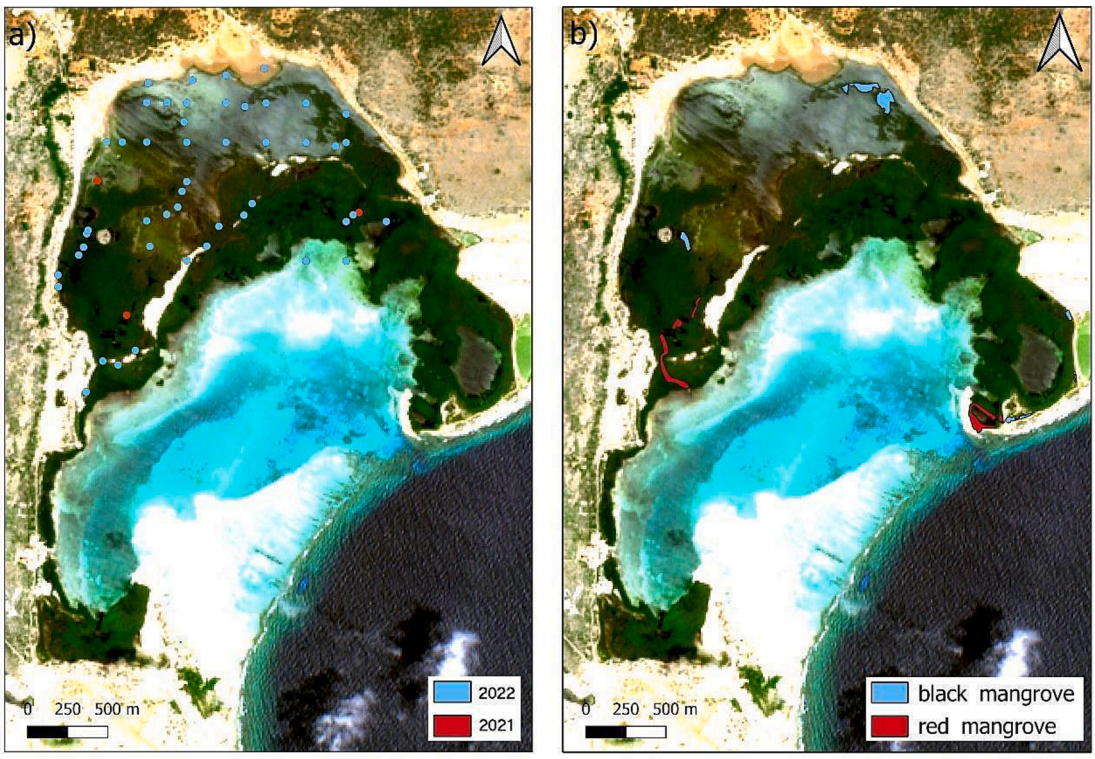

Fig. 3. (a) Sampling sites within Lac Bay, Bonaire, where PAIe was determined *in situ* (n = 51) (b) Homogeneous areas defined in field observations on 14 March 2023 for red mangrove (*R. mangle*) (n = 5) and black mangrove (*A. germinans*) or black mangrove (n = 7). (For interpretation of the references to colour in this figure legend, the reader is referred to the web version of this article.)

from shore and islands larger than 100 km^2 in area, thus including small islands such as Bonaire.

Sentinel-2 images coincident with fieldwork dates were downloaded from the Sentinel Data Hub at the 2A level, Bottom Of Atmosphere reflectance images (BOA) (Table 2). Prior to analysis, these images were resized to focus on the Lac Bay study area (Fig. 1b). Seven Sentinel-2 images were used to find the relationship between *in situ* and satellite data, while only five Sentinel-2 images were used for the creation of the thematic maps and average calculations due to cloud coverage issues. Examining multiple images enhances our methodology's robustness, enabling a more comprehensive assessment of replicability and the identification of seasonal variations.

2.4. Mangrove forest extent and species composition

Mapping the extent and composition of mangrove forests over time is a prerequisite to identifying unwanted changes and developing targeted measures to address these changes in a timely manner. A typical method for mapping vegetation areas using remote sensing is the use of vegetation indices. Vegetation indices use the relationship between different spectral bands to distinguish vegetation from other substrate types.

Table 2
Sentinel-2 images included in the analysis. Due to cloud coverage, Sentinel-2 images registered on 22/04/2022 and 02/05/2022 were only used to evaluate the relationship between satellite and *in situ* data.

Sentinel-2 Date	Acquisition time (UTC)	Satellite	Granule	Season
19/09/2021	15:07:19	S2B	T19PEP	Dry
28/12/2021	15:07:19	S2B	T19PEP	Wet
12/01/2022	15:07:21	S2A	T19PEP	Wet
23/03/2022	15:07:21	S2A	T19PEP	Dry
02/04/2022	15:07:21	S2A	T19PEP	Dry
22/04/2022	15:07:31	S2A	T19PEP	Dry
02/05/2022	15:07:31	S2A	T19PEP	Dry

Some authors reported that conventional vegetation indices are not suitable for mapping mangrove forests, and that their use can present some challenges in distinguishing mangroves from terrestrial vegetation (Winarso et al., 2014). For this reason, some researchers have developed mangrove-specific indices. To map mangrove extent in Lac Bay, Bonaire, we evaluated a traditional vegetation index, the Normalised Difference Vegetation Index (NDVI) (Rouse et al., 1973), and several mangrove-specific indices, namely the Combined Mangrove Recognition Index (CMRI) (Gupta et al., 2018), the Mangrove Forest Index (MFI) (Jia et al., 2019), and the Mangrove Vegetation Index (MVI) (Baloloy et al., 2020) (Table 3). All these indices allow mangrove pixels to be classified by applying a simple threshold. Supervised classification based on Maximum Likelihood (ML) parametric decision rules was also tested, including the 10 m bands. The ML classifier differs from vegetation

Table 3
Mangrove vegetation indices tested in this study, where ρ indicates the reflectance at the specified Sentinel-2 bands.

Vegetation Index	Formula	Reference
Normalised Difference Vegetation Index (NDVI)	NDVI = (ρB8 - ρB4)/(ρB8 + ρB4)	Rouse et al., 1973
Combined Mangrove Recognition Index (CMRI)	CMRI = NDVI - NDWI *where NDWI = (ρB3 - ρB8)/(ρB3 + ρB8)*	Gupta et al., 2018
Mangrove Forest Index (MFI)	MFI = $[(\rho_{\lambda.1} - \rho_{B\lambda.1}) + (\rho_{\lambda.2} - \rho_{B\lambda.2}) + (\rho_{\lambda.3} - \rho_{B\lambda.3}) + (\rho_{\lambda.4} - \rho_{B\lambda.4})]/4$ $\rho B\lambda i = \rho B12 + (\rho B4 - \rho B12) \times (2190 - \lambda i)/(2190–665)$ *where the ρλ is the reflectance of the band centre of λ, and i ranged from 1 to 4; 1, 2, 3, 4 are the centre wavelengths at B5 (705 nm), B6 (740 nm), B7 (783 nm) and B8a (865 nm), respectively.*	Jia et al., 2019
Mangrove Vegetation Index (MVI)	MVI = (ρB8 - ρB3)/ ρB11 - ρB3)	Baloloy et al., 2020

indices as it assumes that the statistics for each class in each band are normally distributed and calculates the probability that a given pixel belongs to a given class (Bolstad and Lillesand, 1991).

Different training and validation datasets were created for mangrove and non-mangrove areas. The training areas representative of mangrove cover included 30 polygons (355 pixels), while the validation areas included 36 polygons (283 pixels). Training areas for non-mangrove cover included 46 polygons (340 pixels), while validation areas included 22 polygons (338 pixels). Classification accuracy was determined using a confusion matrix (also called error matrix) in which classification results were compared based on the established categories (classes). Commission errors correspond to values predicted in one class but not belonging to that class (false positives), while omission errors were predicted to be in a different class (false negatives).

Once the total extent of the mangrove forest was defined, the differentiation between *A. germinans* and *R. mangle* areas was evaluated. For this purpose, eight Sentinel-2 bands (443 nm − 842 nm) were included in the analysis and areas outside the mangrove forest were masked out. Species-specific training and validation areas were defined using the data acquired during the field campaigns (Fig. 3b). To be statistically representative, the minimum size of training and validation areas should include a minimum of $m + 1$ pixels per category according to (Chuvieco, 2020), with m being the number of bands used in the classification process. As we included eight Sentinel-2 bands, the minimum number of pixels per species category should be nine in our case, which is substantially lower than the number of pixels selected for training and validation that were used in this study for *A. germinans* areas (respectively 70 and 20 pixels) and *R. mangle* areas (respectively 78 and 31 pixels).

To evaluate species separability, two types of classifications were carried out: 1) Maximum Likelihood (ML) and 2) Maximum Likelihood after a Principal Component Analysis (PCA) to remove redundant information before the classification. In both cases, classification accuracy was evaluated using a confusion matrix and the commission and omission errors. Separability analysis using the Jeffries-Matusita (J-M) distance analysis was also applied using the training and validation areas defined for each class. This separability index delivers a value between 0 and 2. Following Vaiphasa et al. (2005), a threshold of ≥ 1.90 was used to define if both classes can be differentiated.

2.5. Biophysical variables: Leaf area Index (LAI)

LAI has been derived from remote sensing data using two main approaches: physics-based approaches and empirical approaches. Empirical approaches generally model the relationship between *in situ* determined LAI and vegetation indices that enhance vegetation while minimising background soil reflectance or atmospheric effects (Huete et al., 2012). The modelled relationship is then used to create thematic maps of LAI using remote sensing imagery. To estimate LAI, most of these optical methods usually assume that leaves have infinitesimal size and are randomly distributed, which is referred to as effective LAI (LAI_e) (e.g., Chen et al., 2005). More complex approaches have been developed in recent years, including physics-based approaches and radiative transfer models, which have proven successful in various environments such as semi-arid regions or agricultural fields (Qui et al., 2000; Haboudane et al., 2004; Wang et al., 2013). Physics-based approaches are based on radiative transfer models and show great flexibility in retrieving variables. However, these models need auxiliary information to parametrize the model, which may not be always available and has an associated risk of oversimplifying the plant cover architecture (Delegido et al., 2011). In this study, we modelled the empirical relationship between a vegetation index (NDVI) and *in situ* LAI_e measurements and validated the physics-based Simplified Level-2 Prototype Processor (SL2P) implemented in the Sentinel Application Platform (SNAP).

2.5.1. LAI empirical approach

Previous studies have evaluated the empirical relationship between LAI and various vegetation indices and have shown that NDVI generally provides the best results (Soudani et al., 2006; Kamal et al., 2016). Considering these studies, NDVI values were extracted from the sites where LAI_e was measured *in situ*, and the relationship was modelled using both a linear function (equation 2) and a non-linear function (equation 3) derived from equation 10 reported by Baret and Guyot (1991).

$$LAI_e = a \cdot NDVI + b \tag{2}$$

$$LAI_e = -\frac{ln\frac{NDVI-a}{b-a}}{k} \tag{3}$$

Model selection was based on Akaike's information criterion (AIC) (Burnham & Anderson, 2002). Parameter estimates, R^2-values, and P-values of the most parsimonious model were reported, with the most parsimonious model being the model with the fewest parameters within 2 ΔAIC of the top model (Burnham & Anderson, 2002). P-values < 0.05 were considered significant. Statistical analyses were performed in R statistical software (R Core Team, 2023, version 4.3.0).

2.5.2. LAI physics-based approach

The SL2P algorithm (Weiss et al., 2020), implemented as open source in SNAP, can provide several biophysical variables of vegetation, including LAI. SL2P uses artificial neural networks (ANNs) trained with radiative transfer simulations from the coupled Leaf Optical Properties Spectra (PROSPECT) model (Jacquemoud and Baret, 1990; Féret et al., 2008) and the Scattering by Arbitrarily Inclined Leaves (SAIL) model (Verhoef, 1984; 1985). The PROSPECT model describes leaf properties on canopy reflectance, while the SAIL model describes the influence of canopy structure. Two spatial resolutions of Sentinel-2 bands, 10 m and 20 m, are considered in SNAP for the generation of the biophysical products, but only the 10 m bands were used in this study. Specific neuronal networks are trained for Sentinel-2A and Sentinel-2B due to their particular spectral response, but both training databases share the same simulation cases regarding model inputs. SL2P does not account for foliage clumping, so their retrievals correspond to LAI_e. Detailed information on the SL2P algorithm can be found in the theoretical-based algorithm document (Weiss et al., 2020).

The SL2P algorithm has been described as generic (Weis et al., 2020), but although some validation experiments have been conducted at different sites and periods (e.g., Djamai et al., 2019; Hu et al., 2020; Brown et al., 2021), a large validation effort is still required to cover different vegetation canopies. This validation effort is particularly needed for mangroves, where only a single published document from Vietnam was found (Binh et al., 2022).

The accuracy of the SL2P algorithm was evaluated using the Bias Diagnostic Error (BDE, see equation 4) and the Root-Mean-Square Error (RMSE, see equation 5). The BDE reflects the tendency to overestimate or underestimate the *in situ* values (resulting in negative or positive bias values, respectively). The RMSE indicates the quality of the predictions, and its value shifts towards zero as quality improves.

$$BDE = \sum_{i=1}^{N} \frac{\rho_{observed} - \rho_{predicted}}{N} \tag{4}$$

$$RMSE = \sqrt{\sum_{i=1}^{N} \frac{(\rho_{observed} - \rho_{predicted})^2}{N}} \tag{5}$$

2.6. Biophysical variables: Net Primary Productivity (NPP)

Models for Net Primary Productivity (NPP) require specific measurements in the field and associated complex analysis. Given the difficulty of conducting field campaigns in mangrove forests and the lack of specific data in this study, we applied a simple empirical model to obtain

an estimate of NPP in our study areas. The selected model defined by equation 6 was chosen for its simplicity and its use in previous studies (e.g., English et al., 1994; Karmaker, 2006):

$$NPP = A{\cdot}d{\cdot}LAI_e \quad (6)$$

where A is the average photosynthetic rate (gC m^{-2} leaf area hr^{-1}) for all leaves in the canopy, d corresponds to day length (hr), and LAI_e is the effective leaf area index estimated for each 10 m pixel of Sentinel-2 data. For mangroves with high soil salinity in the dry season, we have used A = 0.216 gC m^{-2} hr^{-1} (Edwards, 1997) while day length in Bonaire averages about 12 h. Due to the lack of values for A in the wet season, the model was only applied to the dry season. To understand how the uncertainty in the NDVI-based LAI_e predictions translate to our NPP predictions, we have used the following formulas (Equations 7 and 8) to calculate the lower (lcl) and upper (ucl) 95 % confidence limits for NPP:

$$lcl(NPP) = A{\cdot}\ d{\cdot}\ lcl(LAI_e) \quad (7)$$

$$ucl(NPP) = A{\cdot}d{\cdot}ucl(LAI_e) \quad (8)$$

3. Results

3.1. Mapping mangrove extent and species composition

When using vegetation indices developed specifically for mapping mangrove forests, the results were unsatisfactory. Visual assessment of results based on MFI and MVI indices showed confusion between mangroves and surrounding substrates, especially water, probably because these indices have been developed and tested in regions with different environmental conditions and mangrove species than those on Bonaire. Given the similar performance of NDVI and CMRI and considering that NDVI is one of the most used indices in mangrove remote sensing (Tran et al., 2022), NDVI was selected for mapping the mangrove extent in Lac Bay. Several threshold values from NDVI $\geq$ 0.2 to NDVI $\geq$ 0.4 at 0. 05 intervals were evaluated, and results were visually assessed, selecting 0.3 as the one producing the best results.

The accuracy of the NDVI mapping (threshold of NDVI $\geq$ 0.3) was evaluated using a confusion matrix. The confusion matrix showed an overall average accuracy of 93.67 %, while the mangrove class reached an accuracy percentage of 97.17 %, indicating good agreement between observed and predicted values. However, differences were found between the dry and wet seasons, with lower overall accuracies for images acquired in the wet season (Table 4). The average accuracy of the mangrove class was estimated to be 97.2 %, while the commission and omission errors had average values of 9.44 % and 2.82 %, respectively. These errors indicated that the extent of the mangrove forest was generally overestimated. Commission errors were higher during the wet season compared to the dry season (Table 4). Based on the NDVI, the extent of the mangrove forest in Lac Bay varied between 240.34 ha and 271.94 ha, depending on the date the satellite image was taken (Table 4).

Visual comparison of the NDVI results for images from the wet and dry seasons showed that the NDVI results are influenced by some seasonal events that cause local variations in the bay. For example, during the wet season, a strong NDVI signal is detected in a small patch of the northern part of Lac Bay, which was classified as mangrove forest (Fig. 4b, c). However, this isolated patch is not detected during the dry season (Fig. 4a, d, e). In addition, in the wet season, a strong vegetation signal is sometimes detected by NDVI in the small lagoon in the southwestern part of Lac Bay (Fig. 4b), which was never detected in the dry season. The seasonal presence of holopelagic *Sargassum spp*. rafts in the southwest of Lac Bay may also explain some of the observed seasonal variability in NDVI at certain sites, as was probably the case for the Sentinel-2 image acquired in March 2022 (Fig. 4d) and to a lesser extent in April 2022 (Fig. 4e). The highest estimations were obtained in the image registered on 28/11/2021 where a patch with a strong vegetation signal was detected in the northern part of the bay and in the small lagoon (Fig. 4b). However, these values can be considered overestimated due to the local processes described above.

Supervised classification methods such as Maximum Likelihood were also evaluated for mapping the mangrove forest extent. The confusion matrix (Table 4) showed an overall mean accuracy of 98.62 %, which is higher compared to NDVI (i.e. 93.68 %). The mangrove class mean achieved a value of 98.42 % and commission and omission errors of 1.24 % and 1.58 %, respectively, indicating less confusion between mangrove and non-mangrove classes than when classification is based on NDVI. Using the classification based on ML, the extent of mangrove forest ranged from 213.46 ha to 238.80 ha, depending on the image, and showed higher values in the wet season. Visual analysis of the supervised ML classification results showed that the patches identified by NDVI in the northern part of the bay in the wet season were also present in the supervised classification results, confirming the presence of a substrate with a strong vegetation signal (Fig. 4 g,h). Supervised classification results showed less confounding effects with other vegetation and urban areas and did not detect any vegetation signal in the small lagoon in the southwestern part of the bay (Fig. 4g). Given these considerations, the supervised classification based on ML was the preferred method for mapping mangrove extent in Lac Bay.

Once the extent of mangrove cover was determined, the ability to distinguish between *R. mangle* and *A. germinans* was examined. Separability analysis based on the Jeffries-Matusita distance showed an average value of 1.95. This value was higher than 1.90 in all the analysed images, indicating sufficient power to distinguish both mangrove species. These results were supported by the spectral signatures for each mangrove species that were extracted using the training and validation areas (Fig. 5). Whereas the spectral signatures for both *R. mangle* and *A. germinans* showed a common peak at 560 nm, the signatures in the red edge and infrared region differed, especially from the 705 nm spectral band onwards (Fig. 5b).

On average, using a PCA before the ML-based classification of

Table 4
Overall accuracies and commission and omission errors resulting from NDVI and Maximum Likelihood (ML) classifications, as well as the estimated extent of mangrove forest in hectares (ha) for each image for each classification method.

Classification method	Date	Season	Overall Accuracy %	Mangrove class %	Commission error %	Omission error %	Extent (ha)
NDVI	19/09/2021	Dry	94.45	97.57	8.45	2.43	251.27
	28/12/2021	Wet	91.86	97.57	12.83	2.43	271.94
	12/01/2022	Wet	92.45	97.57	11.87	2.43	267.53
	23/03/2022	Dry	94.81	96.59	7.03	3.41	240.98
	02/04/2022	Dry	94.81	96.56	7.03	3.41	240.34
	Mean NDVI		93.68	97.17	9.44	2.82	254.41
ML	19/09/2021	Dry	99.84	99.65	0.00	0.35	213.46
	28/12/2021	Wet	98.56	98.03	0.85	1.97	226.28
	12/01/2022	Wet	99.52	100.00	1.05	0.00	238.80
	23/03/2022	Dry	97.12	95.49	1.17	4.51	217.64
	02/04/2022	Dry	98.07	98.94	3.11	1.06	215.15
	Mean ML		98.62	98.42	1.24	1.58	222.27

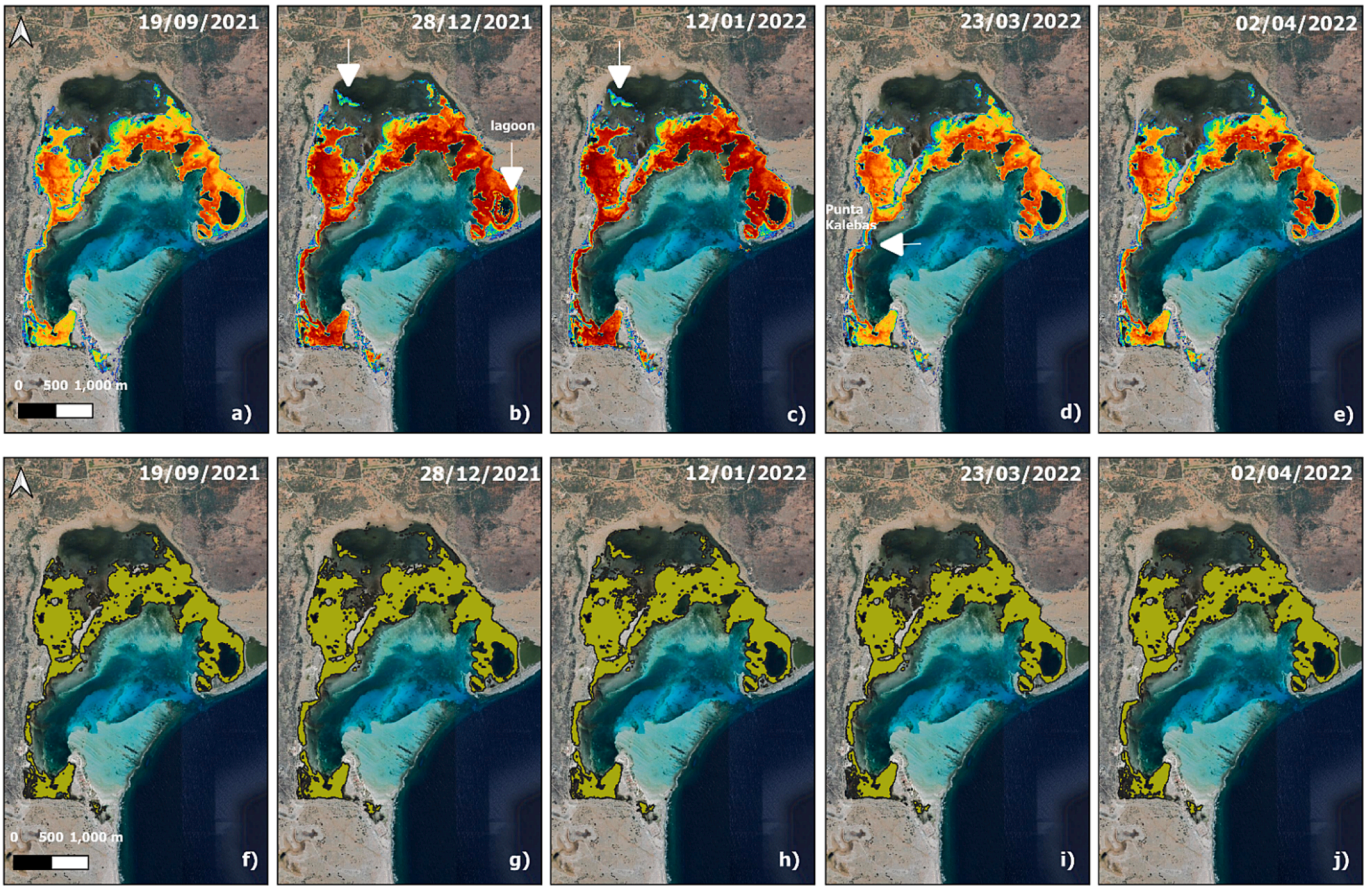

Fig. 4. Extent of mangrove forest based on NDVI estimates (a – e) and supervised classification (f – j). White arrows in (b) and (c) indicate areas with a strong chlorophyll signal, while the arrow in (d) marks the possible presence of pelagic *Sargassum spp.* rafts that seasonally accumulate in this part of the bay.

mangrove species improved results by increasing overall accuracies (Table 5). The highest overall accuracies (100 %) were obtained for the images acquired in the early dry season on 23 March 2023 and 2 April 2022 (Table 5). These results were supported by spectral signatures that showed a clear difference between species (Fig. 5b). Commission and omission errors were also considerably reduced when PCA was applied before ML. Commission errors for *A. germinans* were higher than omission errors, indicating an overestimation of the black mangrove class, while omission errors for *R. mangle* indicated a slight underestimation of this class (Table 5, Fig. 5a).

3.2. Biophysical variables: Leaf area Index (LAI)

3.2.1. LAI empirical approach

Comparison of a linear function and a non-linear function to model the relationship between NDVI derived from Sentinel-2 imagery and *in situ* measured LAI_e showed that the linear function provided the most parsimonious model (linear function: AIC = 140.7, df = 3; non-linear function AIC = 142.64, df = 4). Using a linear function, we observed a significant positive relationship between NDVI and LAI_e ($p < 0.001$, $R^2 = 0.74$; Fig. 6), described as $LAI_e = -0.0282 + 4.516 * NDVI$.

Subsequently, LAI_e thematic maps were produced for the mangrove-covered area in Lac Bay using the obtained linear regression model and NDVI values derived from the Sentinel-2 images. Only images completely free of clouds were used (n = 3 and n = 2 for dry and wet seasons, respectively; Table 6). Estimated mean values of LAI_e in Lac Bay ranged from 3.37 to 3.85 depending on the image, with significantly higher values in the wet season compared to the dry season (*t*-test, $p < 0.05$, Table 6, Fig. 7). LAI_e values showed a zonal distribution with increasing values when moving from the backwaters towards the seashore (Fig. 7).

3.2.1.1. Validation of LAI physical-based approach. Comparison between the *in situ* values of LAI_e and SL2P-derived LAI_e showed a strong relationship ($R^2 = 0.67$, Fig. 8). Yet, BSE was positive (BSE = 0.41) indicating an underestimation of LAI_e values based on the SL2P model (Fig. 8).

The mean LAI_e values for the mangrove cover in Lac Bay (Bonaire) were also estimated using the SL2P model (Table 7) but were much lower than the ones produced by the LAI_e empirical model, confirming the underestimation of LAI_e values by the SL2P model.

3.3. Biophysical variables: Net Primary Productivity (NPP)

Using the empirically derived model products for LAI_e and the model described in equation 5, NPP thematic maps were produced for Lac Bay (Fig. 9). Using this model, a mean NPP value of 8.82 ± 1.46 g Cm^{-2} d^{-1} was obtained for the three Sentinel-2 images that were registered in the dry season (Table 8).

The obtained maps show a zonal distribution of NPP values in Lac Bay, with the highest values in the mid-west and on the east side of the bay, near the seashore (see Fig. 9).

4. Discussion

4.1. Mangrove forest extent and species composition

We evaluated the use of Sentinel-2 satellite images to map the extent and species composition of a small mangrove forest, using Lac Bay, Bonaire, as a case study. Results showed that a threshold value of NDVI

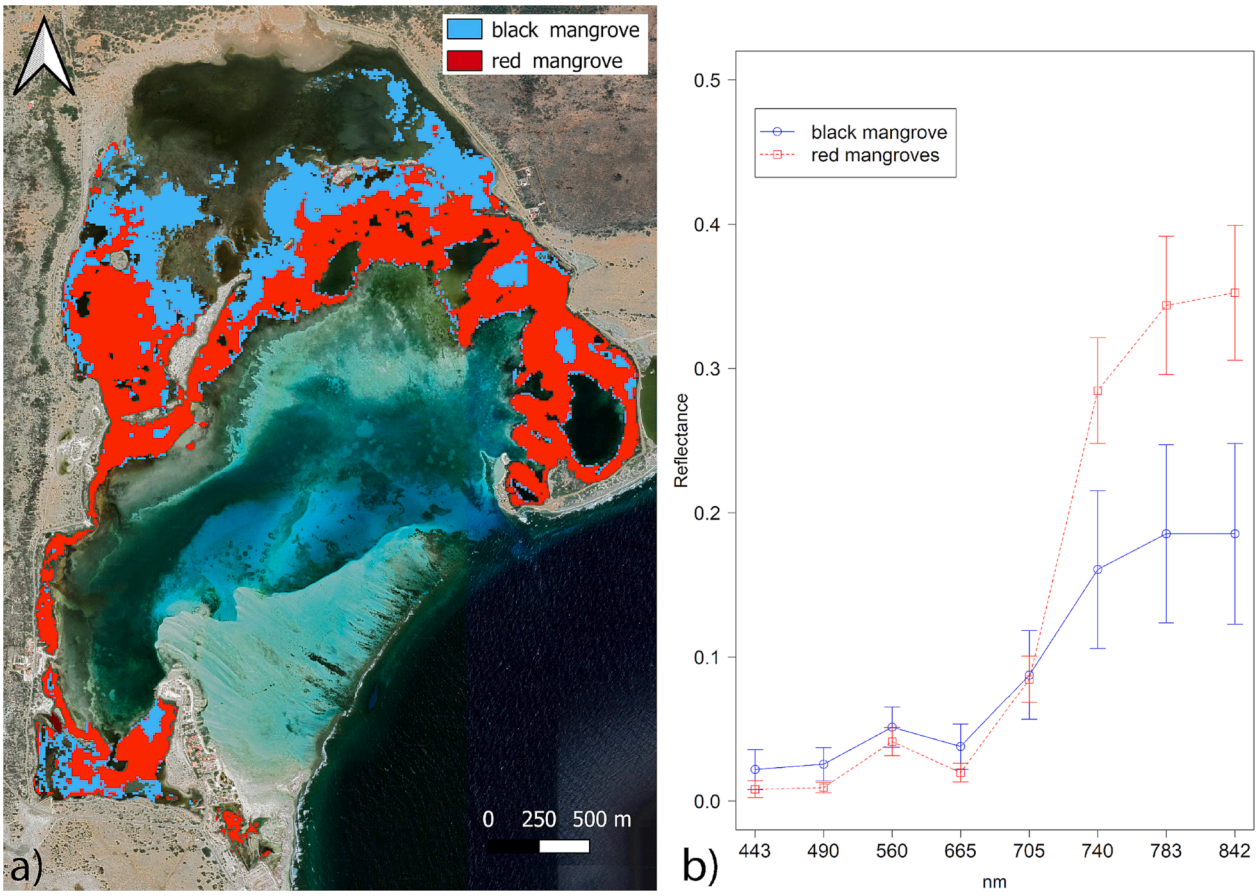

Fig. 5. (a) Thematic map of the distribution of the black mangrove *A. germinans* (in blue) and the red mangrove *R. mangle* (in red) in Lac Bay derived from the Sentinel-2 image registered on 23/03/2022. (b) Species-specific mean (± standard deviation) spectral signatures extracted from the Sentinel-2 images using the training and validation areas defined during field campaigns.

≥ 0.3 provided accurate maps of the mangrove forest extent. However, some seasonal variability in mangrove cover was observed based on this vegetation index. For example, during the wet season, NDVI elucidated a small patch with a strong chlorophyll signal in the Northern backwaters of Lac Bay, within the range of NDVI values classified as mangrove forest (Fig. 4 b,c). These patches correspond to an opportunistic seagrass species (i.e., *Ruppia maritima*) that is known to grow in this area during the wet season when salinity levels drop, after which it dies off when salinity increases again during the following dry season (pers. obs.). Another strong vegetation signal was identified by NDVI in the small lagoon in the southwestern part of Lac Bay during the wet season (Fig. 4b). Due to the inaccessibility of this lagoon, we could not determine the cause of this effect. Possible causes could be natural processes in the lagoon, such as rain-induced algal blooms, or satellite image effects, such as sun glint, even though they could not be visually detected in the image. NDVI results may also have been influenced by holopelagic *Sargassum spp*. rafts that have been drifting into the bay seasonally since 2018 (López-Contreras et al., 2021). Most likely, the influence of holopelagic *Sargassum spp*. can be observed in the Sentinel-2 image acquired on 23 March 2022, when *Sargassum* spp. rafts were known to be concentrated near Punta Kalebas (pers. obs.), exactly at the location where NDVI identified a strong vegetation signal (Fig. 4d). Together, these local environmental factors may have influenced the NDVI results, which consequently tend to overestimate the extent of the mangrove forest, especially during the wet season (i.e., October to January) and during the *Sargassum* spp. influx season (i.e., March to August). As such, we conclude that NDVI can be effectively used to map the extent of small mangrove forests but that knowledge about local environmental conditions is needed to select the most optimal period for which remote sensing images are acquired to do so. For long-term NDVI-based monitoring of the extent of the small mangrove forests in Lac Bay, Bonaire, it is therefore recommended to use remote sensing images that are acquired in September (i.e., after the holopelagic *Sargassum spp*. influx season and before the wet season).

Regarding mapping the extent of small mangrove forests, classification based on Maximum Likelihood estimation (ML) provided more robust results than the classification based on NDVI. For example, mapping based on ML did not show the strong vegetation signal detected by NDVI in the lagoon. After eliminating the area of strong vegetation signal detected in the northern part, which does not correspond to the mangrove forest, classification based on ML identified an average extent of 222.26 ha of mangrove forest, of which 136.03 ha was classified as *R. mangle* and 77.10 ha as *A. germinans*. Note that the remaining unclassified mangrove area (~9 ha) most likely was dominated by *L. racemosa*, although this needs validation in the field. These numbers correspond to the average of the five Sentinel-2 images analysed in this study. A recent study that used two Sentinel-2 images taken on 30 October 2018 and 8 January 2019 reported that the extent of the mangrove area in Lac Bay covered 247 ha, of which 199 ha was identified as intact mangroves and 48 ha as degraded mangroves (Senger et al., 2021). If we compare these data with the estimations obtained in this study in 2022, for example for the image registered on 23 March 2022, we obtain a loss of 10 % in the extent of the mangrove area in just over 3 years (i.e., between 8 January 2019 and 23 March 2022). Although this potential decline in mangrove cover is in line with the general trend of mangrove loss reported for the Caribbean region over the last two decades (Bunting et al., 2022), comparison of our results with those reported by Senger et al. (2021) should be taken with care, as

Table 5
Overall accuracies and commission and omission errors for *A. germinans* and *R. mangle* obtained for each Sentinel-2 image. ML = Maximum Likelihood, PCA + ML = Principal Component Analysis previously applied to the ML supervised classification.

Classification method	Date	General Overall Accuracy %	Accuracy *A. germinans* %	Accuracy *R. mangle* %	Commission error *A. germinans* %	Commission error *R. mangle* %	Omission error *A. germinans* %	Omission error *R. mangle* %	Extent (ha) *A. germinans*	Extent (ha) *R. mangle*
ML	19/09/2021	95.35	100.00	93.55	14.29	0.00	0.00	6.45	64.15	148.93
	28/12/2021	90.70	100.00	87.10	25.00	0.00	0.00	12.90	72.95	140.15
	12/01/2022	90.70	100.00	87.10	25.00	0.00	0.00	12.90	79.45	133.63
	23/03/2022	93.02	100.00	90.32	20.00	0.00	0.00	9.68	73.18	139.90
	02/04/2022	93.02	100.00	90.32	20.00	0.00	0.00	9.68	73.18	139.90
	Mean ML	92.56	100.00	89.68	20.86	0.00	0.00	10.32	72.58	140.50
PCA + ML	19/09/2021	95.34	100.00	93.55	14.29	0.00	0.00	6.45	73.52	139.56
	28/12/2021	95.35	100.00	93.55	14.29	0.00	0.00	6.45	72.95	140.15
	12/01/2022	95.34	100.00	93.55	14.29	0.00	0.00	6.45	80.65	132.65
	23/03/2022	100.00	100.00	100.00	0.00	0.00	0.00	0.00	75.96	137.12
	02/04/2022	100.00	100.00	100.00	0.00	0.00	0.00	0.00	82.41	130.67
	Mean PCA + ML	97.21	100.00	96.13	8.57	0.00	0.00	3.87	77.10	136.03

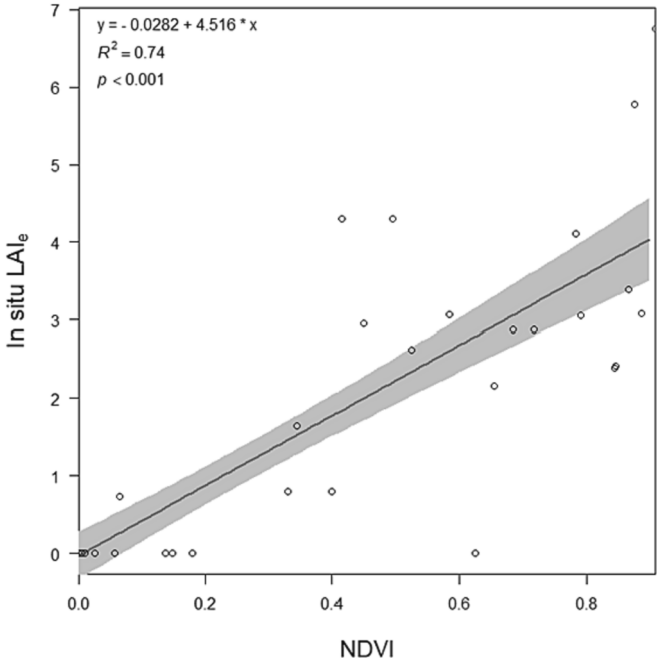

Fig. 6. Scatterplot of *in situ* effective Leaf Area Index (LAI_e) as a function of NDVI (n = 51). The mean (solid line) and 95 % confidence intervals (grey area) are estimated by the most parsimonious linear model.

Table 6
Mean, Standard deviation (SD), and Maximum (Max) LAI_e values estimated for Lac Bay (Bonaire) using the linear regression model developed in this study with NDVI as explanatory variable.

Date	Season	Mean LAI_e	SD LAIe	Max LAI_e
19/09/2021	Dry	3.37	0.55	4.17
28/12/2021	Wet	3.79	0.56	4.48
12/01/2022	Wet	3.85	0.59	4.49
23/03/2022	Dry	3.39	0.56	4.15
02/04/2022	Dry	3.45	0.58	4.25

different classification methods were used (i.e., Random Forest compared to ML in this study).

Using a commercially available Worldview-2 image with 2 m resolution acquired on 28 October 2010, Davaasuren and Meesters (2012) estimated the mangrove area in Lac Bay to be 293.60 ha, of which 121.10 ha consisted of *R. mangle*, 58.10 ha of *A. germinans* and 123.4 ha of mixed mangrove forest (Table 9). Considering our mean estimation (i.e., 222.26 ha), this would suggest that the extent of the mangrove forest in Lac Bay has declined by 24.3 % (i.e., 71.3 ha) in 11.5 years only. Yet, this potential mangrove loss between 2010 and 2022 should also be taken with care as the satellite source and the classification methodology used in both studies were different. Unlike Davaasuren and Meesters (2012), the extent of mixed mangrove populations was not estimated in this study, so that we were unable to compare our results for species-specific mangrove extent with their results. Although at a lower rate, mangrove losses were also reported between 1961 and 1996, during which an area of 82 ha died-off, most of which occurred in the northern

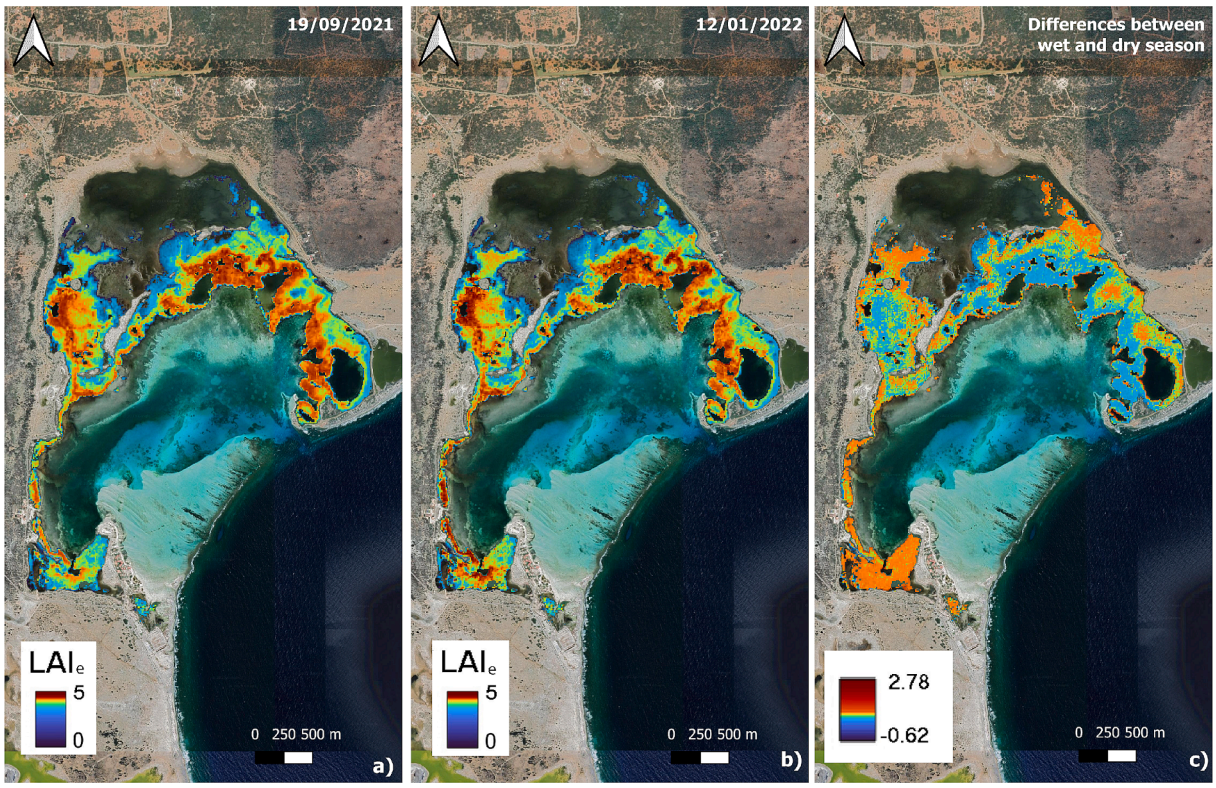

Fig. 7. Maps of estimated LAI_e for Lac Bay (Bonaire) based on NDVI for satellite images recorded on (a) 19/09/2021 (dry season) and (b) 12/01/2022 (wet season), and (c) differences in LAI_e between these two images. Symbology of the three maps is in quartile mode to enhance visualisation.

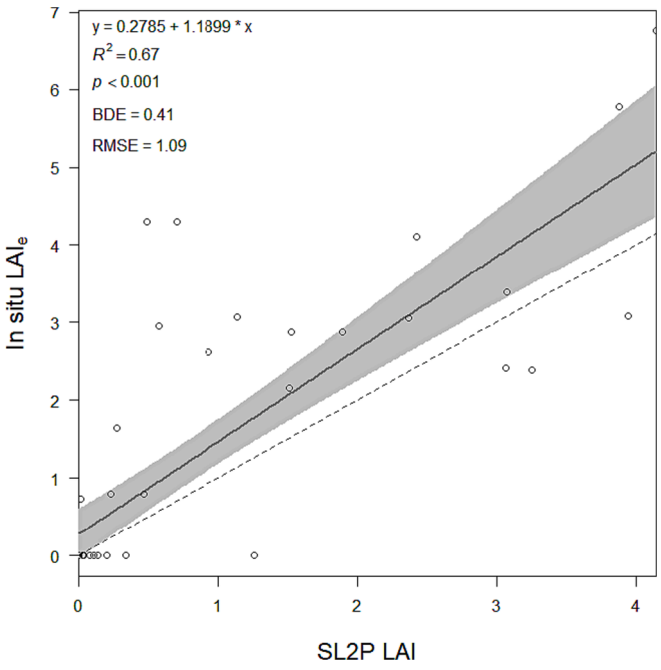

Fig. 8. Scatterplot of *in situ* effective Leaf Area Index (LAI_e) as a function of modelled SL2P LAI data. The mean (solid line) and 95 % confidence intervals (grey area) are estimated by the linear model, while the dashed line reflects an y = x relationship. Bias Diagnostic Error (BDE) and the Root-Mean-Square Error (RMSE) are also included.

backwaters of Lac Bay (Erdmann and Scheffers, 2006). The main cause for this local mangrove die-off was suggested to be endogenous sediment production and terrestrial erosion-induced sedimentation, which

Table 7
Mean, Standard Deviation (SD) and Maximum (Max) values of LAI_e for Lac Bay (Bonaire) based on the SL2P model.

Date	Season	Mean SL2P LAI_e	SD SL2P LAI_e	Max SL2P LAI_e
19/09/2021	Dry	2.24	1.02	4.80
28/12/2021	Wet	2.79	1.13	5.28
12/01/2022	Wet	2.84	1.13	5.55
23/03/2022	Dry	2.23	1.04	4.70
02/04/2022	Dry	2.36	1.09	4.99

gradually turned the backwaters of Lac Bay into hypersaline anaerobic flats with high water residence times, unfavourable for mangrove growth and survival (Wösten, 2013, Debrot et al., 2019). However, over the same period, Erdmann and Scheffers (2006)) also reported seaward expansion of the mangrove forest, covering an area of 81 ha at the expense of the lagoon. This ongoing process leads to a reduction in the surface area of marine habitat within the bay, and expansion of hypersaline tidal flat area in the back of the bay at the expense of mangrove forest, and is considered to pose a significant risk to the baýs long-term biodiversity and ecosystem functionality (Debrot et al., 2019).

The distribution map of *R. mangle* and *A. germinans* in Lac Bay showed a clear zonal distribution (Fig. 5a), which is in accordance with De Freitas et al. (2005) and Davaasuren and Meesters (2012). *R. mangle* grows in frequently or permanently flooded areas near the seaward margins of the mangrove forest, while *A. germinans* grows at higher elevation areas with low water content, as found in the northern backwaters of Lac Bay. The ability to discriminate between both species using Sentinel-2 probably comes from the spectral behaviour of mangrove leaves. This fact is mainly determined by the presence of pigments such as chlorophyll, which causes a reflectance peak at 560 nm and two minima at 443–490 nm and 665 nm corresponding to chlorophyll absorption. *A. germinans* leaves have higher chlorophyll concentrations (Chl a + Chl b) compared to those of *R. mangle* (Zhang et al., 2012),

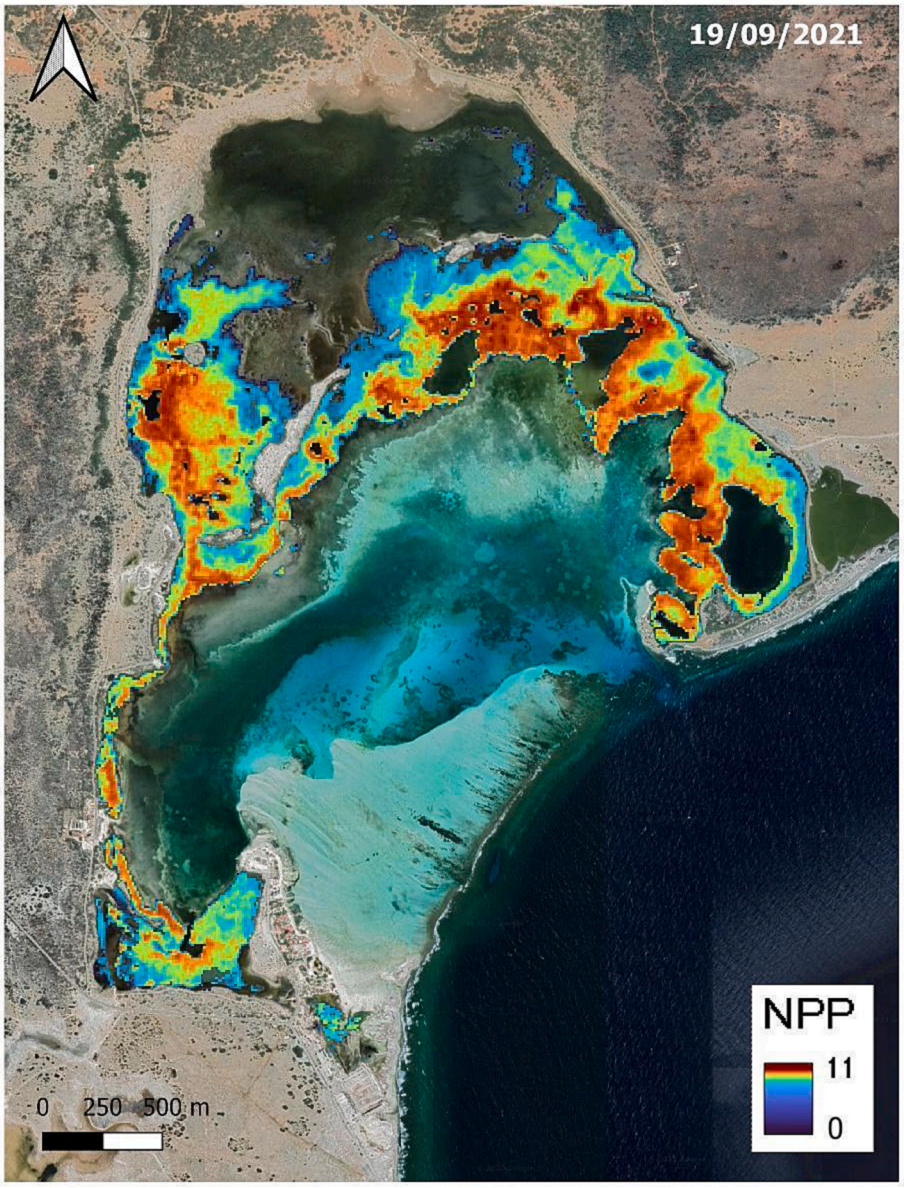

Fig. 9. NPP values (g Cm^{-2} d^{-1}) of Lac Bay on 19/09/2021 (end of the dry season). The symbology of the map is in quartile mode to enhance visualisation.

Table 8
Mean NPP values (g C m^{-2} d^{-1}), standard deviation (SD), minimum (Min NPP), and maximum (Max NPP) values estimated for Lac Bay for three satellite images collected in the dry season, as well as the predicted lower 95% confidence limit (lcl) and upper 95% confidence limit (ucl) based on equation 6 and 7.

Date	Mean NPP (satellite image)	SD (satellite image)	Min / Max NPP (satellite image)	Predicted lcl	Predicted ucl
19/09/2021	8.73	1.42	0/ 10.80	7.17	9.30
23/03/2022	8.78	1.46	0/ 10.76	7.17	9.30
02/04/2022	8.94	1.51	0/ 11.02	7.38	9.57

Table 9
Overview of remote sensing derived extent of mangrove forest (ha) reported for different dates and mangrove species in Lac Bay, Bonaire. ML = Maximum Likelihood, RF = Random forest.

Study	Satellite	Image year	Method	Total extent (ha)	*R. mangle* (ha)	*A. germinans* (ha)	Mixed areas (ha)
This study	Sentinel-2	2021, 2022	ML	222.26	136.03	77.10	–
Senger et al., 2021	Sentinel-2	2018, 2019	RF	247.00	–	–	–
Davaasuren and Meesters, 2012	Worldview-2	2010	ML	293.60	121.10	58.10	123.40

while *R. mangle* leaves contain higher concentrations of carotenoids and pigments called anthocyanins, which give them a reddish colour. Leaf structure is also different in both species, *R. mangle* leaves are large and elongated compared to *A. germinans* leaves that are relatively small and more oval. These species-specific leaf characteristics may explain the observed species-specific reflectance signatures in the visible and infrared regions (see Fig. 5b). Zhang et al. (2014) also reported that *A. germinans* leaves tend to have higher reflectance in the visible range, while *R. mangle* leaves have higher reflectance in the near-infrared range. As such, the use of species-specific spectral reflectance signatures seems to be a very promising tool to differentiate between *A. germinans* and *R. mangle* populations (Zhang et al., 2012; Zhang et al., 2014). However, research incorporating radiometric field measurements in Lac Bay is still needed to validate this method.

Given the rapid changes that can occur in the distribution and composition of small mangrove forests, as observed in Lac Bay, there is a clear need for consistent and structural long-term monitoring of the extent and species composition of the small mangrove forests to timely identify and address possible causes of these changes. Results presented in this study convincingly show that freely available Sentinel-2 images can be used to provide accurate maps of the extent and structure of small mangrove forests. As such, the cost-effective mangrove monitoring method developed in this study seems very suitable for long-term monitoring of the mangrove forest of Lac Bay, Bonaire, and other mangrove forests on small island states with similar species composition (i.e., in the Caribbean) where human and financial resources are limited. The methodology proposed in this study was specifically applied in a semi-arid region, where the presence of vegetation, apart from mangroves, is relatively low. In locations where diverse vegetation types coexist, the interpretable mangrove mapping approach (IMMA) could be useful to mitigate the interference of non-mangrove vegetation, enhancing the accuracy of mangrove mapping in these cases (Zhao et al., 2023a).

Recent advancements in classification techniques, such as the incorporation of explainable machine learning (XAI), are widely recognized as pivotal for the effective deployment of artificial intelligence (AI) models (Arrieta et al., 2020). Future work incorporating XAI could help enhance the predictive accuracy of classification results, ensuring a decision-making process that is understandable and interpretable (Arrieta et al., 2020). Recognizing interpretability as an essential design factor can further improve the implementability of AI models, contributing to impartial decision-making and ensuring that only meaningful variables influence the model's output (Arrieta et al., 2020). Dual-temporal Sentinel-2 images combining Sentinel-2 and Sentinel-1 data could also give new insights incorporating physical properties to the classification analysis, such as roughness and dielectricity (Zhao et al., 2023b). Further exploration of XAI approaches, which approximate complex models by self-interpretable models, would be key in the future for improving mangrove canopy identification and mapping using satellite data. However, it is important to note that implementing these advanced techniques requires a certain level of skills and expertise, which may be lacking in small island states. Acquiring and applying these capabilities demands specialised knowledge that can represent a potential challenge for the effective utilization of such technologies in regions with limited resources. Thus, addressing this gap in skills and expertise is crucial for ensuring the successful implementation of advanced AI models in smaller, less-resourced areas.

4.2. Remote sensing indicators of mangrove forest condition

In this study, we show that Sentinel-2-derived LAI data can be used to map LAI_e accurately in the small mangrove forest of Lac Bay, where mean LAI_e values were estimated to be 3.57 with maximum average values of 4.31. The minimum LAI_e values in our case were 0, as some non-vegetated pixels could be included in the classification (commission errors). In any case, our values align with those documented in other studies conducted in the Caribbean region. For example, using Landsat imagery, Green et al. (1997) found a mean LAI value of 3.96 (range 0.8 – 7.0) for mangroves growing on the Caicos Bank, Turks, and Caicos Islands. These authors have used similar steps for LAI calculation (equation 1 of this study), but they do not have apply any correction for woody material. Following these assumptions, the values they are reporting correspond to PAI_e instead of LAI_e. Sherman et al. (2003) reported a mean LAI value of 4.4 (range 2.9 – 5.6) for a mangrove forest in the Dominican Republic. In this case LAI values were derived from allometric relationships.

Our results showed a strong positive relationship between LAI_e and NDVI ($R^2 = 0.75$). As such, the modelled equation for this relationship could potentially be used to derive LAI_e for small mangrove forests with similar species composition (i.e., on other small island in the Caribbean) when NDVI data are available. In other regions of the world where the composition of mangrove species is different, the relationship might not be as strong, for instance due to the species-specific character of the extinction coefficient *k* (Guo et al., 2021). Therefore, if resources allow, it is preferred to adjust the modelled equation based on local species-specific estimates of LAI_e following the approach presented in this study and, if possible, determine the extinction coefficient of the specific species using a terrestrial laser scanning technique (see Zheng and Moskal, 2012). Even though some studies have considered vegetation indices that incorporate red-edge bands to derive LAI (e.g., Delegido et al., 2011), specific works carried out in mangrove forests have reported the best results when NIR bands were used (Guo et al., 2021). Additionally, the extensive and historical application of the NDVI facilitates a higher level of comparability with other studies. Using this empirically derived LAI_e algorithm, we were able to detect seasonal differences in LAI_e, with significantly lower LAI_e values in the dry season compared to the wet season. During the wet season, mangrove forests experience increased rainfall, which results in reduced salinity levels and increased access to freshwater, both favourable for photosynthesis and tree growth, and eventually may have resulted in relatively high LAI_e values compared to the dry season (Jaramillo et al., 2018). Moreover, the wet season is typically associated with higher nutrient availability for mangrove trees due to rainfall-induced run-off of terrestrial sediments and organic matter into the coastal areas where the trees grow (Rahaman et al., 2013).

The performance of the generic algorithm S2LP underestimated our *in situ* obtained LAI_e values for the mangrove forest in Lac Bay, as was reflected by the positive value for BSE (BSE = 0.41). So far, little research has been done to validate S2LP estimates for LAI in mangrove canopies, except for a study by Binh et al. (2022) in Vietnam. These authors reported a positive relationship between *in situ* LAI and SL2P estimates ($R^2 = 0.45$) and an underestimation of LAI values by the model (RMSE = 2.19) without clarifying if their *in situ* values correspond to LAI or LAI_e. Although the LAI_e estimations provided by SL2P in our study were slightly better (e.g., $R^2 = 0.67$, RMSE = 1.09), the error values are still too high to consider the results acceptable. On the other hand, other studies have reported that SL2P LAI retrievals can show poor performance over heterogeneous canopies such as forests and at relatively high LAI values (i.e., LAI > 3) (Brown et al., 2021). Collection of *in situ* LAI data at multiple locations and in various types of mangrove forests (i.e., mangrove fringe forests, over washed mangrove islands, riverine mangrove forests, basin mangrove forests, dwarf mangrove forests) is needed to validate global SL2P-based LAI algorithms and to refine them, if necessary. These will help to better represent LAI for different types of mangrove forests and locations (Gilmore and Snedaker, 1993), providing more accurate estimations.

Furthermore, the application of a lux meter for LAI measurements in mangrove forests remains underexplored and requires some further work for enhancing the reliability of these data. For example, by a comparative analysis of simultaneous measurements from a lux meter and a Photosynthetic Active Radiation (PAR) meter.

The net primary production (NPP), derived from satellite-derived

LAI values, is also a key indicator of ecosystem productivity and can be used directly to assess the function of carbon sequestration or the service of climate regulation (Trégarot et al., 2021). In fact, LAI is an indicator of the amount of photosynthesis that occurs in the canopy, which is moderated by the amount of leaf material in which it can occur. Therefore, a higher LAI generally results in a higher NPP. Without specific data to develop a physics-based NPP model, we decided to evaluate a simple empirical algorithm based on LAI values. Our results for Lac Bay showed an average NPP for the dry season of 8.82 ± 1.46 gC m^{-2} d^{-1}, equivalent to about 118.15 ± 19.56 tCO_2 ha^{-1} yr^{-1}. This means NPP values from Bonaire are much higher than NPP estimates obtained for the mangrove forests of Martinique (37.80 ± 12.85 tCO2 ha^{-1} yr^{-1}) using the NPP MODIS product with 500 m of spatial resolution (Trégarot et al., 2021). Further work is needed to determine if this difference could result from the different spatial resolution in NPP estimations, where low spatial resolution seems to result in lower NPP values, or from the different methodologies employed in both cases (empirically-derived vs physically-based model). The lack of available data on NPP in Lac Bay limits the comparison of our results with other studies in this area. However, studies published in the Caribbean region reported similar values for NPP in mangrove forests. For example, Vega-Rodríguez (2008) reported a mean NPP of 12.6 g Cm^{-2} d^{-1} for monospecific sites of *R. mangle* in La Parguera, Puerto Rico. These results suggest that the model used to derive NPP could provide reliable values and encourage further work to develop more robust models. In the meantime, LAI and NPP values can be used to monitor the productivity of the mangrove forests in Lac Bay and to assess the service of climate regulation, which currently represents 26 260 ± 4 347 tCO_2eq yr^{-1} for the mangrove forests of Lac Bay.

Finally, in Lac Bay, NDVI, LAI_e, and NPP values showed a clear zonal distribution with the highest values in the mid-West and East on the seaward side of the bay and lowest values in the northern landward part of the bay, indicating a degraded condition of the mangrove forest compared to its pioneer front. However, the ecological condition of an ecosystem can only be interpreted in light of a reference system being either the same ecosystem at another point in time or an ecosystem in a similar geomorphic setting but considered pristine (i.e., with low pressures on the system to none). As such, we cannot derive further inference from the results of our study in terms of ecological condition, but our results provide the baseline for future assessments in Bonaire. Furthermore, as discussed above, the use of a NPP indicator in particular, not only allows to estimate the condition of the forest but also provides a direct estimation of the service of climate regulation through the function of carbon sequestration. In the frame of ecosystem services valuation, considering the ecological condition is essential to account for the loss in the quantity and/or quality of a service, as the extent of the mangrove alone does not necessarily reflect this loss (Trégarot et al., 2021). The use of remote sensing imaging thus allows to have both parameters (extent and condition) and, in some cases the production function underlying the service at large spatial and long temporal scales. Moreover, this information is provided more cost-effectively compared to the number of traditional field campaigns necessary to achieve the same results in order to support mangrove management and conservation.

5. Conclusions

This study shows that Sentinel-2 satellites are effective tools for mapping mangrove forests on small tropical islands, providing valuable information for the management of these fragile ecosystems. We used Sentinel-2 data to map the extent of the mangrove forest, species composition, and ecological condition through two biophysical variables: LAI_e and NPP. Our findings indicate that NDVI can be used to accurately map the extent of the small mangrove forest in Lac Bay, if satellite images are captured during the dry season and outside of the main *Sargassum* influx months (e.g., September). In terms of classification accuracy, the Maximum Likelihood algorithm outperformed NDVI as it was not influenced by seasonal processes. By utilising Maximum Likelihood, we estimated the mangrove forest extent in Lac Bay to be 222.3 ha, with 136.0 ha classified as *R. mangle* (red mangroves) and 77.1 ha as *A. germinans* (black mangroves). Furthermore, our study highlights the significance of developing local algorithms to derive values of biophysical variables such as LAI and NPP and supports the effectiveness of NDVI-based algorithms for obtaining LAI values. LAI_e values were significantly higher in the wet season than the dry season, with mean values of 3.82 and 3.40, respectively. Regarding NPP, we obtained a mean NPP of 8.82 ± 1.46 gC m^{-2} d^{-1} during the dry season, equivalent to approximately 139.88 ± 34.37 tCO_2 ha^{-1} yr^{-1} for Lac Bay.

Overall, this study provides a cost-effective method for monitoring the extent, composition, and ecological condition of the small mangrove forest in Lac Bay, Bonaire. This method also has the potential to be extrapolated to other small islands with comparable mangrove forest compositions. Its implementation is particularly relevant for SIDS where data scarcity is common due to limited human capacity and financial resources, enabling informed decision-making for the management and protection of their valuable mangrove ecosystems.

CRediT authorship contribution statement

Gema Casal: Writing – review & editing, Writing – original draft, Funding acquisition, Formal analysis, Data curation, Conceptualization. **Ewan Trégarot:** Writing – review & editing, Writing – original draft, Funding acquisition, Data curation, Conceptualization. **Cindy C. Cornet:** Writing – review & editing, Funding acquisition. **Tim McCarthy:** Writing – review & editing, Funding acquisition. **Matthijs van der Geest:** Writing – review & editing, Writing – original draft, Funding acquisition, Formal analysis, Data curation, Conceptualization.

Declaration of competing interest

The authors declare that they have no known competing financial interests or personal relationships that could have appeared to influence the work reported in this paper.

Data availability

Data will be made available on request.

Acknowledgements

This work was supported by the European Union's Horizon 2020 research and innovation programme under grant agreement No 869710 "Marine Coastal Ecosystems Biodiversity and Services in a Changing World" (MaCoBioS) to all authors and by the Netherlands Ministry of Agriculture, Nature and Food Quality under research project BO-43-117-007 to M. van der Geest. The authors wish to thank Femke van der Drift for helping with the collection of the 2022 field data. We further thank Sabine Engel from Mangrove Maniacs and STINAPA rangers and additional staff, for their advice, cooperation, and assistance during our field campaigns. We would also like to thank the two anonymous reviewers for their valuable comments that improved the overall quality of the paper.

References

Arrieta, A.B., Díaz-Rodríguez, N., Del Ser, J., Bennetot, A., Tabik, S., Barbado, A., García, S., Gil-López, S., Molina, D., Benjamins, R., Chatila, R., Herrera, F., 2020. Explainable artificial intelligence (XAI): concepts, taxonomies, opportunities and challenges toward responsible AI. Inf. Fusion 58, 82–115.

Azhdari, Z., Sardooi, E.R., Bazrafshan, O., Zamani, H., Singh, V.P., Saravi, M.M., Ramezani, M., 2020. Impact of climate change on net primary production (NPP) in

south Iran. Environ. Monit. Assess. 192, 1–16. https://link.springer.com/article/10.1007/s10661-020-08389-w.
Baloloy, A.B., Blanco, A.C., Sta. Ana, R.R.C., Nadaoka, K., 2020. Development and Application of a New Mangrove Vegetation Index (MVI) for Rapid and Accurate Mangrove Mapping. ISPRS J. Photogramm. Remote Sens. 166, 95–117. 10.1016/j.isprsjprs.2020.06.001.
Baret, F., Guyot, G., 1991. Potential and limits of vegetation indices for LAI and APAR assessment. Remote Sensing of Environment 35 (2), 161–173.
Barr, J.G., Engel, V., Fuentes, J.D., Fuller, D.O., Kwon, H., 2013. Modelling light use efficiency in a subtropical mangrove forest equipped with CO_2 eddy covariance. Biogeociences 10, 2145–2158. https://doi.org/10.5194/bg-10-2145-2013.
Binh, N.A., Hauser, L.T., Hoa, P.V., Thao, G.T.P., An, N.N., Nhut, H.S., Phuong, T.A., Verrelst, J., 2022. Quantifying mangrove leaf area index from Sentinel-2 imagery using hybrid models and active learning. Int. J. Remote Sens. 43 (15–16), 5636–5657. https://doi.org/10.1080/01431161.2021.2024912.
Bolstad, P.V., Lillesand, T.M., 1991. Rapid maximum likelihood classification. Photogramm. Eng. Remote Sensing 57, 67–74.
Brown, L.A., Fernandes, R., Djamai, N., Meier, C., Gobron, N., Morris, H., Canisius, F., Bai, G., Lerebourg, C., Lanconelli, C., Clerici, M., Dash, J., 2021. Validation of baseline and modified Sentinel-2 Level 2 Prototype Processor leaf area index retrievals over the United States. ISPRS J. Photogramm. Remote Sens. 175, 71–87. https://doi.org/10.1016/j.isprsjprs.2021.02.020.
Bryan-Brown, D.N., Connolly, R.M., Richards, D.R., Adame, F., Friess, D.A., Brown, C.J., 2020. Global trends in mangrove forest fragmentation. Sci. Rep. 10 (1), 7117. https://doi.org/10.1038/s41598-020-63880-1.
Bunting, P., Rosenqvist, A., Lucas, R.M., Rebelo, L.-M., Hilarides, L., Thomas, N., Hardy, A., Itoh, T., Shimada, M., Finlayson, C.M., 2018. The global mangrove watch—a new 2010 global baseline of mangrove extent. Remote Sensing 10 (10), 1669. https://doi.org/10.3390/rs10101669.
Bunting, P., Rosenqvist, A., Hilarides, L., Lucas, R.M., Thomas, N., Tadono, T., Worthington, T.A., Spalding, M., Murray, N.J., Rebelo, L.M., 2022. Global mangrove extent change 1996–2020: Global Mangrove Watch version 3.0. Remote Sens. 14, 3657. https://doi.org/10.3390/rs14153657.
Burnham, K.P., Anderson, D.R., 2002. Model selection and multi-model inference: a practical information-theoretic approach. Springer-Verlag, New York, NY.
CBS, 2021. Trends in the Caribbean Netherlands 2021. © Statistics Netherlands, The Hague/Heerlen/Bonaire, 2021.
Chapin FS III, Eviner VT., 2003. Biogeochemistry of terrestrial net primary production. In Treatise on Geochemistry. Volume 8: Biogeochemistry, ed. WH Schlesinger.
Chen, J.M., Cihlar, J., 1996. Retrieving leaf area index of boreal conifer forests using Landsat TM images. Remote Sens. Environ. 55 (2), 153–162. 10. 1016/0034-4257(95)00195-6.
Chen, J.M., Black, T.A., 1992. Defining leaf area index for non-flat leaves. Plant, Cell Environ. 15, 421–429. https://doi.org/10.1111/j.1365-3040.1992.tb00992.x.
Chen, J.M., Menges, C.H., Leblanc, S.G., 2005. Global mapping of foliage clumping index using multi-angular satellite data. Remote Sensing of Environment 97 (4), 447–457. https://doi.org/10.1016/j.rse.2005.05.003.
Chuvieco, E., 2020. Fundamentals of Satellite Remote Sensing. CRC Press, Boca Raton, FL, An Environmental Approach. Third Edition.
Clough, B.F., Ong, J.E., Gong, W.K., 1997. Estimating leaf area index and photosynthetic production in canopies of the mangrove *Rhizophora apiculata*. Marine Ecology Progress Series 159, 285–292.
Davaasuren, N., Meesters, H.W.G., 2012. Extent and health of mangroves in Lac Bay Bonaire using satellite data. Wageningen-IMARES Report C190/11.
De Freitas, J.A., Nijhof, B.S.J., Rojer, A.C., Debrot, A.O., 2005. Landscape ecological vegetation map of the island of Bonaire (Southern Caribbean). Royal Netherlands Academy of Arts and Sciences, Amsterdam, p. 64.
De Freitas, J.A., Nijhof, B.S.J., Rojer, A.C., Debrot, A.O., 2014. Landscape ecological vegetation map of the island of Bonaire (Southern Caribbean). Royal Netherlands Academy of Arts and Sciences, Amsterdam.
De Grave, C., Pipia, L., Siegmann, B., Morcillo-Pallarés, P., Rivera-Caicedo, J.P., Moreno, J., Verrelst, J., 2021. Retrieving and Validating Leaf and Canopy Chlorophyll Content at Moderate Resolution: A Multiscale Analysis with the Sentinel-3 OLCI Sensor. Remote Sens. 13, 1419. https://doi.org/10.3390/rs13081419.
De Meyer, K., 1998. In: CARICOMP—Caribbean Coral Reef, Seagrass and Mangrove Sites, p. 347 p..
Debrot, A.O., Hylkema, A., Vogelaar, W., Prud'homme van Reine, W.F., Engel, M.S., van Hateren, J.A., Meesters, E.H., 2019. Patterns of distribution and drivers of change in shallow seagrass and algal assemblages of a non-estuarine Southern Caribbean mangrove lagoon. Aquatic Botany 159 (January), 103148. https://doi.org/10.1016/j.aquabot.2019.103148.
Delegido, J., Verrelst, J., Alonso, L., Moreno, J., 2011. Evaluation of Sentinel-2 red-edge bands for empirical estimation of green LAI and chlorophyll content. Sensors 11, 7063–7081.
DES, 2018. Monitoring and Sampling Manual: Environmental Protection (Water) Policy. Department of Environment and Science Government, Brisbane.
Djamai, N., Fernandes, R., Weiss, McNaairn, H., Goïta, K., 2019. Validation of the Sentinel Simplified 2 Product Prototype Processor (SL2P) for mapping cropland biophysical variable using Sentinel-2/MSI and Landsat-8/OLI data. Remote Sens. Environ. 225, 416-430. 10.1016/j.rse.2019.03.020.
Drusch, M., Del Bello, U., Carlier, S., Colin, O., Fernandez, V., Gascon, F., Hoersch, B., Isola, C., Laberinti, P., Martimort, P., Meygret, A., Spoto, F., Sy, O., Marchese, F., Bargellini, P., 2012. Sentinel–2: ESA's optical high-resolution mission for GMES operational services. Remote Sensing of Environment 120, 25–36.
Dullaart, J.C.M., van Manen, S., 2022. An assessment of the impacts of climate change on coastal inundation on Bonaire. Water and Climate Risk, Institute for Environmental Studies (IVM), R-22/05 pp. 55.
Edwards, A. J., 1997. Assessing Mangrove Leaf Area Index (LAI) using CASI Airborne Imagery, 162 – 276. In A. J. Edwards (Eds). Applications of satellite and airborne image data to coastal Management. Coastal region and small island papers 4. UNESCO.
English, S., Wilkinson, C., Baker, V., 1994. Survey Manual for Tropical Marine Resources. Australian Institute of Marine Science, Townsville, p. 368.
Erdmann, W., Scheffers, A., 2006. Mangrove Population of Lac (Bonaire) 1961 and 1996. Universität Duisburg-Essen - Institut für Geographie.
Feka, N.Z., Morrison, I., 2017. Managing mangroves for coastal ecosystems change: a decade and beyond of conservation experiences and lessons for and from west-central Africa. J. Ecol. Nat. Environ. 9, 99–123.
Féret, J.-B., François, C., Asner, G.P., Gitelson, A.A., Martin, R.E., Bidel, L.P.R., Ustin, S. L., le Maire, G., Jacquemoud, S., 2008. PROSPECT-4 and 5: advances in the leaf optical properties model separating photosynthetic pigments. Remote Sens. Environ. 112, 3030–3043. https://doi.org/10.1016/j.rse.2008.02.012.
Field, C.B., Behrenfeld, M.J., Randenson, J.T., Falkowski, P., 1998. Primary production of the biosphere: integrating terrestrial and oceanic components. Science 281, 237-240. https://doi.org /10.1126/science.281.5374.237.
Flores de Santiago, F. J., 2013. Multiple approaches for assessing mangrove biophysical and biochemical variables using in situ and remote sensing techniques. Electronic Thesis and Dissertation Repository. 1345. https://ir.lib.uwo.ca/etd/1345.
Gao, F., Anderson, M.C., Kustas, W.P., Wang, Y., 2012. Simple method for retrieving leaf area index from Landsat using MODIS leaf area index products as reference. J. Appl. Remote Sens. 6 (1), 063554.
GCOS, 2011. Systematic observation requirements for satellite-based products for climate. https://www-cdn.eumetsat.int/files/2020-04/pdf conf p50 s7 01 bojinski p.pdf.
Gilmore, R.G., Snedaker, S.C., 1993. Mangrove forests. Biodiversity of the Southeastern United States: lowland terrestrial communities. John Wiley & Sons, New York, pp. 165–198.
Giri, C., Ochieng, E., Tieszen, L., Zhu, Z., Singh, A., Loveland, T., Masek, J., Duke, N., 2011. Status and Distribution of Mangrove Forests of the World Using Earth Observation Satellite Data. Glob. Ecol. Biogeogr. 20 (1), 154–159. https://doi.org/10.1111/j.1466-8238.2010.00584.x.
Goetz, S.J., Prince, S.D., Small, J., Gleason, A.C.R., 2000. Interannual variability of global terrestrial primary production: Results of a model driven with satellite observations. J. Geophys. Res. Atmos. 105 (D15), 20077–20091. https://doi.org/10.1029/2000JD900274.
Goldberg, L., Lagomasino, D., Thomas, N., Fatoyinbo, T., 2020. Global declines in human-driven mangrove loss. Glob Chang. Biol. 26, 5844–5855. https://doi.org/10.1111/gcb.15275.
Gower, S.T., Kucharik, C.J., Norman, J.M., 1999. Direct and indirect estimation of leaf area index, fAPAR, and net primary production of terrestrial ecosystems. Remote Sensing of Environment 70, 29–51.
Green, E.P., Mumby, P.J., Edwards, A.J., Clark, C.D., Ellis, A.C., 1997. Estimating leaf area index of mangroves from satellite data. Aquat. Bot. 58, 11–19. https://doi.org/10.1016/S0304-3770(97)00013-2.
Green, E.P., Mumby, P.J., Edwards, A.J., Clark, C.D., Ellis, A.C., 1998. The assessment of mangrove areas using high resolution multispectral airborne imagery. J. Coast. Res. 14 (2), 433–443.
Guo, X., Wang, M., Jia, M., Wang, W., 2021. Estimating Mangrove Leaf Area Index Based on Red-Edge Vegetation Indices: A Comparison among UAV, WorldView-2 and Sentinel-2 Imagery. Int. J. Appl. Earth Obs. Geoinf. 103, 102493.
Gupta, K., Mukhopadhyay, A., Giri, S., Chanda, A., Datta Majumdar, S., Samanta, S., Mitra, D., Samal, R.N., Pattnaik, A.K., Hazra, S., 2018. An index for discrimination of mangroves from non-mangroves using LANDSAT 8 OLI imagery. MethodsX 5, 1129–1139. https://doi.org/10.1016/j.mex.2018.09.011.
Haboudane, D., Miller, J.R., Pattey, E., Zarco-Tejada, P.J., Strachan, I.B., 2004. Hyperspectral vegetation indices and novel algorithms for predicting green LAI of crop canopies: modelling and validation in the context of precision agriculture. Remote Sens. Environ. 90 (3), 337–352. https://doi.org/10.1016/j.rse.2003.12.013.
Hu, Q., Yang, J., Xu, B., Huang, J., Memon, M.S., Yin, G., Zeng, Y., Zhao, J., Liu, K., 2020. Evaluation of Global Decametric-Resolution LAI, FAPAR and FVC Estimates Derived from Sentinel-2 Imagery. Remote Sens. 12, 912. https://doi.org/10.3390/rs12060912.
Huete, A.R., 2012. Vegetation indices, remote sensing and forest monitoring. Geogr. Compass 6, 295–532. https://doi.org/10.1111/j.1749-8198.2012.00507.x.
IPCC, 2013. The IPCC's Fifth Assessment Report: What's in it for Small Island Developing States? Cambridge University Press, Cambridge, United Kingdom and New York, NY, USA.
Ishtiaque, A., Myint, S.W., Wang, W., 2016. Examining the ecosystem health and sustainability of the worlds largest mangrove forest using multi-temporal MODIS products. Sci. Total Environ. 589–570, 1241–1254. https://doi.org/10.1016/j.scitotenv.2016.06.200.
Jacquemoud, S., Baret, F., 1990. PROSPECT: A model of leaf optical properties spectra. Remote Sens. Environ. 34, 75–91. https://doi.org/10.1016/0034-4257(90)90100-Z.
Jaramillo, F., Licero, L., Åhlen, I., Manzoni, S., Rodríguez-Rodríguez, J.A., Guittard, A., Hylin, A., Bolaños, J., Jawitz, J., Wdowinski, S., Martínez, O., Espinosa, L.F., 2018. Effects of Hydroclimatic Change and Rehabilitation Activities on Salinity and Mangroves in the Ciénaga Grande de Santa Marta, Colombia. Wetlands 38, 755–767. https://doi.org/10.1007/s13157-018-1024-7.

Jia, M., Wang, Z., Wang, C., Mao, D., Zhang, Y., 2019. A new vegetation index to detect periodically submerged Mangrove forest using Single-Tide Sentinel-2 Imagery. Remote Sens. 11, 2043; 10.3390/rs11172043.
Jia, M., Wang, Z., Mao, D., Ren, C., Song, K., Zhao, C., Wang, C., Xiao, X., Wang, Y., 2023. Mapping global distribution of mangrove forests at 10-m resolution. Sci. Bull. 68 (12), 1306–1316. https://doi.org/10.1016/j.scib.2023.05.004.
Kamal, M., Phinn, S., Johansen, K., 2016. Assessment of multi-resolution image data for mangrove area index mapping. Remote Sens. Environ. 176, 242–254. https://doi.org/10.1016/j.rse.2016.02.013.
Karmaker, S., 2006. Study of Mangrove Biomass, Net Primary Production and Species Distribution using remote sensing data. Ph.D. Thesis, Indian Institute of Remote Sensing, Dehradun, India.
López-Contreras, A.M., van der Geest, M., Deetman, B., van den Burg, S.W.K., Brust, G.M. H., de Vrije, G.J., 2021. Opportunities for valorization of pelagic Sargassum in the Dutch Caribbean. WUR Report 2137. https://doi.org/10.18174/543797.
Lu, X., Zhang, L., Chen, Y., Zhang, Y., 2017. Relationships between leaf area index (LAI) and aboveground biomass in different aged stands of mangroves. Ecological Indicators 73, 47–53.
Millennium Ecosystem Assessment, 2005. Mille ecosystems and human well-being: synthesis. Island Press, Washington, DC.
Myneni, R., Knyazikhin, T.Y., Park, T., 2015. MOD15A2H MODIS/Terra Leaf Area Index/FPAR 8-Day L4 Global 500 m SIN Grid VNASA EOSDIS Land Processes DAAC. Available Online. https://doi.org/10.5067/MODIS/MOD15A2H.006 (accessed on 19 April 2023).
Nagelkerken, I., 2007. Are non-estuarine mangroves connected to coral reefs through fish migration? Bulletin of Marine Science 80, 595–607. https://doi.org/10.1016/j.biocon.2005.09.042.
Nilson, T., 1971. A theoretical analysis of the frequency of gaps in plant stands. Agricultural Meteorology 8, 25–38.
Pachavo, G., Murwira, A., 2014. Remote Sensing net primary productivity (NPP) estimation with the aid of GIS modelled shortwave radiation (SWR) in a Southern African savanna. Int. J. Appl. Earth Obs. Geoinf. 30, 217–226. https://doi.org/10.1016/j.jag.2014.02.007.
Parida, B.R., Kumari, A., 2021. Mapping and Modeling Mangrove Biophysical and Biochemical Parameters Using Sentinel-2A Satellite Data in Bhitarkanika National Park. Odisha. Model. Earth Syst. Environ. 7, 2463–2474.
Piao, S.L., Fang, J.Y., Guo, Q., H., 2001. Application of CASA model to the estimation of Chinese terrestrial net primary productivity. Chin. J. Plant Ecol. 25 (5), 603–608.
Qui, J., Kerr, Y.H., Moran, M.S., Weltz, M., Huete, A.R., Sorooshian, S., Bryant, R., 2000. Leaf Area Index estimates using remotely sensed data and BRDF models in a semiarid region. Remote Sens. Environ. 73, 18–30. https://doi.org/10.1016/S0034-4257(99)00113-3.
R Core Team, 2023. R: A Language and Environment for Statistical Computing. R Foundation for Statistical Computing, Vienna, Austria.
Rahaman, S.M.B., Sarder, L., Rahaman, M.S., Ghosh, A.K., Biswas, S.K., Siraj, S.M.S., Huq, K.A., Hasanuzzaman, A.F.M., Islam, S.S., 2013. Nutrient dynamics in the Sundarbans mangrove estuarine system of Bangladesh under different weather and tidal cycles. Ecol. Process 2, 29. https://doi.org/10.1186/2192-1709-2-29.
Rouse, J.W., Haas, R.H, Schell, J.A., Deering, D.W., 1973. Monitoring vegetation systems in the Great Plains with ERTS (Earth Resources Technology Satellite). In Proceedings of the Third Earth Resources Technology Satellite Symposium, Greenbelt, ON, Canada, 10-14 December, 309-317 pp.
Rull, V., 2023. Rise and Fall of Caribbean Mangroves. Science of Total Environment 885, 163851.
Senger, D.G., Saavedra Hortua, D.A., Engel, S., Shnurawa, M., Moosdorf, N., Gillis, L.G., 2021. Impacts of wetland dieback on carbon dynamics: A comparison between intact and degraded mangroves. Sci. Total Environ. 753, 141817 https://doi.org/10.1016/j.scitotenv.2020.141817.
Sherman, R.E., Fahey, T.J., Martinez, P., 2003. Spatial patterns of biomass and aboveground net primary productivity in a mangrove ecosystem in the Dominican Republic. Ecosystems 6, 384–398. https://doi.org/10.1007/s10021-002-0191-8.
Shrestha, S., Miranda, I., Kumar, A., Pardo, M.L.E., Dahal, S., Rashid, T., Remillard, C., Mishra, D.R., 2019. Identifying and forecasting potential biophysical risk areas within a tropical mangrove ecosystem using multi-sensor data. Int. J. Appl. Earth Obs. Geoinf. 74, 281–294. https://doi.org/10.1016/j.jag.2018.09.017.
Slijkerman, D., van der Geest, M., Debrot, A.O., 2019. Nexus interventions for small tropical islands: case study Bonaire: Water. Wageningen Marine Research. https://edepot.wur.nl/471563.
Soudani, K., François, C., le Maire, G., Le Dantec, V., Dufrêne, E., 2006. Comparative analysis of IKONOS, SPOT, and ETM+ data for leaf area index estimation in temperate coniferous and deciduous forest stands. Remote Sens. Environ. 102, 161–175. https://doi.org/10.1016/j.rse.2006.02.004.
Tran, T.V., Reef, R., Zhu, X., 2022. A review of spectral indices for mangrove remote sensing. Remote Sens. 14, 4868. https://doi.org/10.3390/rs14194868.
Trégarot, E., Caillaud, A., Cornet, C.C., Taureau, F., Catry, T., Cragg, S.M., Failler, P., 2021. Mangrove ecological services at the forefront of coastal change in the French overseas territories. Science of the Total Environment 763, 143004.
Vaiphasa, C., Ongsomwang, S., Vaiphasa, T., Skidmore, A.K., 2005. Tropical mangrove species discrimination using hyperspectral data: a laboratory study. Estuar. Coast. Shelf Sci. 65, 371–379. https://doi.org/10.1016/j.ecss.2005.06.014.
van Moorsel, G.W.N.M., Meijer, A.J.M., 1993. Base-Line Ecological Study van het Lae op Bonaire. Bureau waardenburg BV, Holland, p. 120.
Vega-Rodríguez, M., 2008. Estimating primary productivity of red mangroves in southwestern Puerto Rico from remote sensing and field measurements. Master of Science in Marine Science, University of Puerto Rico, Mayaguez Campus.
Verhoef, W., 1984. Light scattering by leaf layers with application to canopy reflectance modeling: the SAIL model. Remote Sens Environ. 16, 125–141. https://doi.org/10.1016/0034-4257(84)90057-9.
Verhoef, W., 1985. Earth observation modeling based on layer scattering matrices. Remote Sens Environ. 17, 165–178.
Waiyasusri, K., 2021. Monitoring the Land Cover Changes in Mangrove Areas and Urbanization using Normalized Difference Vegetation Index and Normalized Difference Built-up Index in Krabi Estuary Wetland, Krabi Province, Thailand. Appl. Ecol. Environ. Res. 43(3), 1–16. 10.35762/AER.2021.43.3.1.
Wang, L., Dong, T., Zhang, G., Niu, Z., 2013. LAI retrieval using PROSAIL model and optimal angle combination of multi-angular data wheat. IEEE J. Sel. Top. Appl. Earth Obs. Remote Sens. 6, 1730–1736. https://doi.org/10.1109/JSTARS.2013.2261474.
Wang, L., Jia, M., Ying, D., Tian, J., 2019. A review of remote sensing for mangrove forests: 1956–2018. Remote Sens. Environ. 231, 111223 https://doi.org/10.1016/j.rse.2019.111223.
Weis, M., Baret, F., Jay, S., 2020. S2ToolBox Level 2 products LAI, FAPAR, FCOVER Version 2.0 EMMAH-CAPTE, INRAe Avignon, France https://hal.inrae.fr/hal-03584016/document Last accessed 28/11/2022.
Winarso G., Purwanto A. D., 2014. Evaluation of Mangrove Damage Level Based on Landsat 8 Image. International Journal of Remote Sensing and Earth Sciences 11(2), 105-116. 10.30536/j.ijreses.2014.v11.a2608.
Wösten, J.H.M., 2013. Ecological rehabilitation of Lac Bonaire by wise management of water and sediments. Wageningen, Alterra, Alterra Report 2448, 40 pp.
Yan, H., Wang, S.Q., Billesbach, D., Oechel, W., Zang, J.H., Meyers, T., Martin, T.A., Matamala, R., Baldocchi, D., Bohrer, G., Dragoni, D., Scott, R., 2012. Global estimation of evapotranspiration using leaf area index-based surface energy and water balance model. Remote Sens. Environ. 124, 581–595. https://doi.org/10.1016/j.rse.2012.06.004.
Zhang, C., Liu, Y., Kovacs, J.M., Flores-Verdugo, F., Flores de Santiago, F., Chen, K., 2012. Spectral response to varying levels of leaf pigments collected from a degraded mangrove forest. J. Appl. Remote Sens. 6, 063501–063502. https://doi.org/10.1117/1.JRS.6.063501.
Zhang, C., Kovacs, J.M., Flores-Verdugo, F., Flores de Santiago, F., 2014. Separating mangrove species and conditions using laboratory hyperspectral data: a case study of a degraded mangrove forest of the Mexican Pacific. Remote Sens. 6, 11673–11688. https://doi.org/10.3390/rs61211673.
Zhao, C., Jia, M., Wang, Z., Mao, D., Wang, Y., 2023a. Identifying mangroves through knowledge extracted from trained random forest models: An interpretable mangrove mapping approach (IMMA). ISPRS Journal of Photogrammetry and Remote Sensing 201, 209–225. https://doi.org/10.1016/j.isprsjprs.2023.05.025.
Zhao, C., Jia, M., Wang, Z., Mao, D., Wang, Y., 2023b. Toward a better understanding of coastal salt marsh mapping: A case from China using dual-temporal images. Remote Sensing of Environment 295, 113664.
Zheng, G., Moskal, L.M., 2012. Spatial variability of terrestrial laser scanning based leaf area index. International Journal of Applied Earth Observation and Geoinformation 19, 226–237.